SORPTION OF C$_8$ AROMATICS ON MCM-41

A THESIS SUBMITTED TO
THE GRADUATE SCHOOL OF NATURAL AND APPLIED SCIENCES
OF
MIDDLE EAST TECHNICAL UNIVERSITY

BY

BARAA ABBAS ALI

IN PARTIAL FULFILLMENT OF THE REQUIREMENTS
FOR
THE DEGREE OF MASTER OF SCIENCE
IN
CHEMICAL ENGINEERING

MAY 2010

Approval of the thesis:

SORPTION OF C$_8$ AROMATICS ON MCM-41

submitted by **BARAA ABBAS ALI** in partial fulfillment of the requirements for the degree of **Master of Science in Chemical Engineering Department, Middle East Technical University**.

Prof. Dr. Canan Özgen   _____
Dean, Graduate School of **Natural and Applied Sciences**

Prof. Dr. Gürkan Karakaş   _____
Head of Department, **Chemical Engineering**

Prof. Dr. Hayrettin Yücel   _____
Supervisor, **Chemical Engineering, METU**

Prof. Dr. Gürkan Karakaş   _____
Co-Supervisor, Chemical Engineering, METU

Examining Committee Members:

Prof. Dr. Deniz Üner   _____
Chemical Engineering Dept., METU

Prof. Dr. Hayrettin Yücel   _____
Chemical Engineering Dept., METU

Prof. Dr. Gürkan Karakaş   _____
Chemical Engineering Dept., METU

Prof. Dr. Suna Balcı   _____
Chemical Engineering Dept., Gazi University

Assoc. Prof. Dr. Halil Kalıpçılar   _____
Chemical Engineering Dept., METU

Date: May 31, 2010

I hereby declare that all information in this document has been obtained and presented in accordance with academic rules and ethical conduct. I also declare that, as required by these rules and conduct, I have fully cited and referenced all material and results that are not original to this work.

Name, Last name: Baraa Abbas Ali

Signature:

ABSTRACT

SORPTION OF C$_8$ AROMATICS ON MCM-41

Baraa Abbas Ali
M.Sc., Department of Chemical Engineering
Supervisor : Prof. Dr. Hayrettin Yücel
Co-Supervisor : Prof. Dr. Gürkan Karakaş

May 2010, 97 pages

The discovery of MCM-41 materials have attracted substantial research attention due to the remarkable features of these materials including a narrow pore size distribution, high surface area, high pore volume, and high thermal and hydrothermal stability, as well as, parallel hexagonal arrangement of uniform cylindrical pores without pore channel intersection. These well-defined structural characteristics make them ideal media to study the adsorption, catalysis, ion exchange, and separation.

MCM-41 sample used in this study was synthesized in (Chemical Engineering Department, Gazi University). The MCM-41 was synthesized by using sodium silicate (0.0705 mol, 27% Silica) as a source of silica and surfactant cetyltrimethylammoniumbromides (CTMABr) (0.036 mol) as template. A characteristic feature of this direct hydothermal synthesis was relatively long synthesis time (96 hour at 120°C).

MCM-41 was characterized by using XRD, and nitrogen physisorption analysis techniques. The characteristic peak in the low-angle region

corresponding to $2\theta = 2.406°$ was obtained for MCM-41 sample indicating high structural ordering of the MCM-41sample. The BET, surface area was found as (492.2 m^2/g), with an average pore diameter (25 Å).

In this study the sorption equilibrium of C$_8$ aromatics (p-xylene, m-xylene, o-xylene, and ethylbenzene) on MCM-41 at different temperatures (30°C, 50°C, 65°C, 80°C) was investigated by using an automated gravimetric electrobalance system. It was found that the amounts of each sorbate (p-xylene, m-xylene, o-xylene, and ethylbenzene) adsorbed at a given relative pressure on MCM-41 decreased when the temperature of the adsorption isotherms increases.

The adsorption isotherms were type V, according to IUPAC isotherm classification due to the mesoporous nature of the MCM-41 sample. The hysteresis are associated with condensation-evaporation within a narrow distribution of mesopores with each adsorption isotherms. It was shown that as the temperature for the adsorption isotherms increases the size of hysteresis decreases for each sorbate. The volume of sorbates (V_p) were obtained from the mass uptake at maximum relative pressure by taking the normal liquid density at the adsorption temperature for all sorbates. These values are significantly lower than that obtained from low-temperature nitrogen isotherm. The reason of this difference is that the density of the adsorbed phase is unlikely to be exactly the same as that of the liquid adsorptive and curvature of some isotherms at high relative pressure leads to uncertainty in the location of the upper limit for pore filling.

Keywords: MCM-41, adsorption, C$_8$ aromatics.

ÖZ

C_8 AROMATİKLERİN MCM-41 ÜZERİNE SORPSIYONU

Baraa Abbas Ali
Yüksek Lisans, Kimya Mühendisliği Bölümü
Tez Yöneticisi : Prof. Dr. Hayrettin Yücel
Ortak Tez Yöneticisi: Prof. Dr. Gürkan Karakaş

Mayıs 2010, 97 sayfa

MCM-41 malzemelerinin keşfi, bu malzemelerin dar gözenek genişliği dağılımı, yüksek yüzey alanı, yüksek termal ve hidrotermal kararlılığı ve kanal gözenek kesişimi olmayan, paralel altıgen geometride düzenli silindirik gözeneklere sahip olma gibi önemli özellikleri sayesinde araştırmacıların ilgisini çekmiştir. İyi tanımlanmış bu yapısal özellikleri, bu malzemeleri adsorpsiyon, katalizör, iyon değişimi ve ayrıştırma çalışmaları için uygun kılmaktadır.

Çalışmada kullanılan MCM-41 örneği (Gazi Üniversitesi Kimya Mühendisliği Bölümü) sentezlenmiştir. MCM-41 sentezi, silika kaynağı olarak sodyum silikat (0.0705 mol, 27% Silika) ve şablon olarak yüzey etkin setiltrimetilamonyumbromür (CTMABr) (0.036 mol) kullanılarak gerçekleştirilmiştir. Bu doğrudan hidrotermal sentez metodunun bir özelliği de görece uzun sentez süresidir. (120°C'de 96 saat).

Sentezlenen MCM-41, XRD ve azot adsorpsiyonu, analiz teknikleri kullanılarak karakterize edilmiştir. MCM-41 örneği için XRD karakteristik piki MCM-41 örneğinin yüksek yapısal düzenini işaret eden şekilde düşük-açı bölgesine denk gelen 2θ= 2.406° da gözlenmiştir.

BET, yüzey alanı (492.2 m^2/g) ve ortalama gözenek çapı (25 Å) olarak bulunmuştur.

Bu çalışmada C$_8$ aromatiklerin (p-ksilen, m-ksilen, o-ksilen, ve etilbenzen) MCM-41 üzerinde, farklı sıcaklıklarda (30°C, 50°C, 65°C, 80°C) sorpsiyonu, otomatik gravimetrik elektroterazi sistemi kullanılarak incelenmiştir. MCM-41 üzerinde, belirli bir bağıl basınç değerinde adsorplanan toplam (p-ksilen, m-ksilen, o-ksilen, ve etilbenzen) miktarları adsorpsiyon izetermlerinin sıcaklığının artmasıyla azalmıştır.

Adsorpsiyon izotermleri, MCM-41 örneğinin mezogözenekli doğasının bir sonucu olarak, IUPAC izoterm sınıflandırmasına göre V tipidir. Histeresis, her adsorpsiyon izotermi için, mezogözenklerin dar dağılımı içinde olan yoğuşma-buharlaşma olayıyla ilintilidir. Her sorbat için histeresis döngülerinin artması ile küçüldüğünü isotermlerin sıcaklıklarının arttığı gözlenmiştir. Sorbat hacmi (V$_P$), normal sıvı yoğunluğunun bütün sorbatlar için adsorpsiyon sıcaklığında alındığı durumda, en yüksek bağıl basınç değerindeki kütle alım kapasitesinden elde edilmiştir. Bu değerler, düşük sıcaklık azot izotermlerinden elde edilen değerlere göre önemli bir düşüklük sergilemektedir. Bu farkın sebebleri absorplanan maddenin absorplanmış fazın yoğunluğunun sıvı fazıyla aynı olmaması ve yüksek bağıl basınç değerlerindeki izotermlerin eğimlerinin, gözenek doluluğu üst limitinin değeri hakkında belirsizliğe sebep olmasıdır.

Anahtar kelimeler: MCM-41, adsorpsiyon, C$_8$ aromatikler.

To my family

ACKNOWLEDGEMENTS

TABLE OF CONTENTS

LIST OF TABLES

LIST OF FIGURES

FIGURES

NOMENCLATURE

MCM   Mobil Composition Matter

Wt   Weight at any time

Wto   Weight of adsorbent at initial time

P   Pressure at any time

Po   Saturation vapour pressure at temperature of adsorption

IGA   Intelligent Gravimetric Analyser

CTMABr   cetyltrimethylammoniumbromides

TEOS   tetraethyl orthosilicate

IUPAC   international union of pure and applied chemistry

CHAPTER 1

INTRODUCTION

1.1 Porous solids

Porous solids have been studied in detail with regard to their technical applications as adsorbents, catalysts, catalyst supports, and ion exchanging agents [1].

According to the IUPAC definition, pore size ranges are divided into three classes [2]:

1- Microporous materials : their pore diameters are less than 2 nm

2- Mesoporous materials : they have pore diameters ranging from 2-50 nm

3- Macroporous materials : they have pore diameters larger than 50 nm

Among the family of microporous materials, the best known members are zeolites. Due to their crystallographically defined pore system, zeolites have a narrow and uniform size distribution in the micropore range [3]. Zeolites are the most widely used catalysts used in chemical industry, such as hydrocarbon conversion (i.e., alkylation, cracking, isomerization), hydrogenation and dehydrogenation, and organic catalysis [4].

1.2 M41S Family

M41S family that is composed of three members, MCM-41, MCM-48 and MCM-50 was first introduced in 1992 by Mobil researchers. MCM denotes to Mobil composition matter whereas the numbers given next to "MCM" name is the batch number. These mesoporous materials having uniform channels ranging from 20 to 100 Å also have high surface area values and each of the M41S family members has different structures. These materials are fundamentally different from zeolites by the fact that the pore walls are amorphous. The ordering lies in the pore arrangements [5]. Surfactant / silica ratio also plays crucial role in the determination of the materials structure. The schematic representation of this property is given in Figure 1.1.
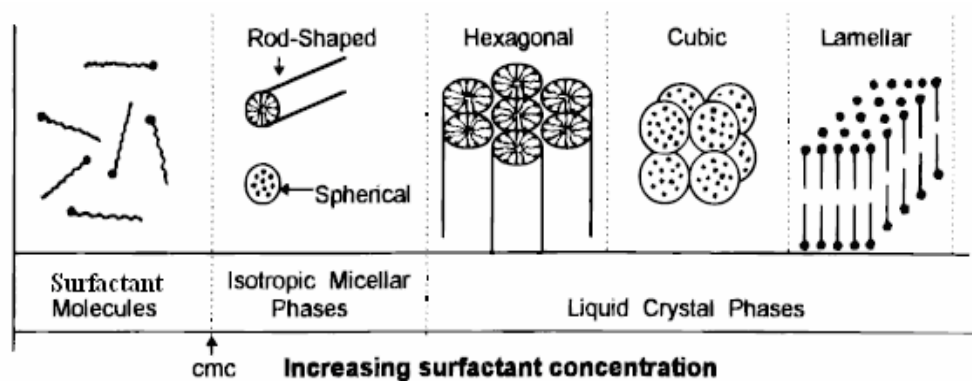
Figure 1.1 Phase sequence of water – surfactant binary system [6]

As seen in the Figure 1.1, when the surfactants are considered in water –surfactant binary system, at low concentrations they energetically exist as monomolecules. Surfactants molecules aggregate together to form micelles in order to decrease the system entropy as the

concentration of surfactant increase. If concentration continues to increase, hexagonal close packed arrays appear, producing the hexagonal phases [7].

The detailed properties of M41S family members are presented in the following sections.

1.2.1 MCM-41

Among all the M41S members, MCM-41 received much more attention than the others because of its interesting unidirectional, hexagonal honeycomb like structure as shown in the schematic representation in the Fig. 1.2(a) and (b)

(a)   (b)
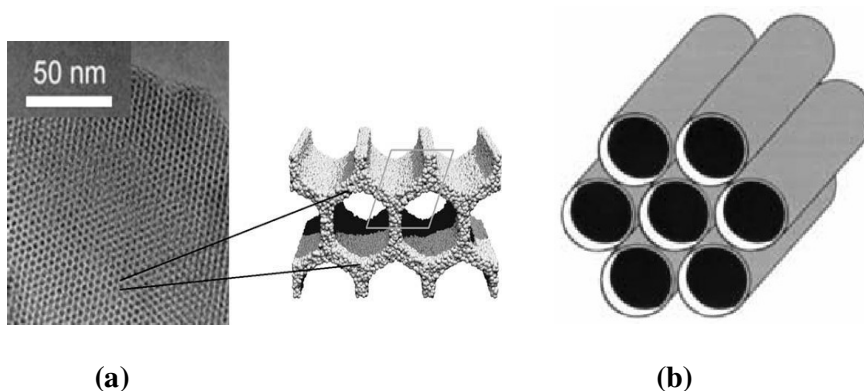
Figure 1.2 (a) TEM image of the MCM-41 [8] (b) the front view of the MCM-41 uni-directional channels [5]

Main components of MCM-41 are a source of silica, structure –directing surfactants, a solvent and acid or base [9]. Moreover, further studies [10] showed that the relative concentration of the species present in the synthesis solutions were very important for the final pore structure. It is also added that the pore diameter of the MCM-41 increases as the chain length of the surfactant increases.

1.2.2 MCM-48

Another M41S family member, MCM-48, is also a good candidate for the catalytic application because of it cubic structure (Figure 1.3) indexed in the space group *Ia3d*, of recently modeled as a gyroid minimal surface [11, 12]. Interesting physical properties of MCM-48 are its high specific surface area up to1600 cm^2/g, specific pore volume up to 1.2 cm^3/g and high thermal stability [13]. The catalytic properties can be adjusted by the incorporation of different metals.
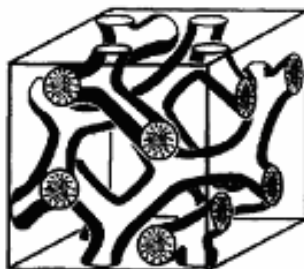
Figure 1.3 the schematic representation of proposed model of MCM-48 [14].

Although MCM-48 has very attractive pore structure, synthesizing it on large scale has some drawbacks. Huo et al. [15] produced MCM-48 using alkoxide-based organic silica sources, such as tetraethylorthosilicate (TEOS) or its homologues. These reagents, however, present significant handling problems (e.g., high toxicity, moisture sensitivity) and are costly, making large-scale synthesis of crystalline MCM-48 by this procedure impractical [69].

1.2.3 MCM-50

Unlike the other M41S family members, MCM-50 has a lamellar arrangement of surfactant and silica layers as shown in the below Figure 1.4. However it is very unstable that the structure of MCM-50 collapses upon calcination and does not give a mesoporous compound [17]

Figure 1.4 The schematic representation of MCM-50 [5]

1.3 Fundamental of adsorption on porous materials

The basic measurement for characterizing the adsorption of gases on solids is the adsorption isotherm which measures the amount adsorbed as a function of the pressure of the sorbate molecules at constant temperature. The first attempt to interpret adsorption isotherms of gases on solids equilibria was introduced by Brunauner, Deming, Deming and Teller (BDDT) in 1940 [18]. These authors classified isotherms into five categories based on the shape of the isotherm. The BDDT classification became the core of the modern IUPAC classification of adsorption isotherms [74, 76]. Variation in isotherm shape reflects difference in the character of the solid surface, the size and shape of the pores, the

porosity and the surface area of the solid and the energy of interaction between the adsorbed molecule and the solid surface. Zeolites are microporous adsorbents; mechanism of adsorption is volume filling of micropores that usually results in a type I isotherm for the most sorbates, where the pores are filled at very low pressure of the adsorbate [19]. Types II and III give adsorption isotherm on macroporous adsorbents with strong and weak affinities, respectively (Figure 1.5).Types IV and V characterize mesoporous adsorbents with strong and weak affinities, respectively. For lower temperatures they show adsorption hysteresis [20].
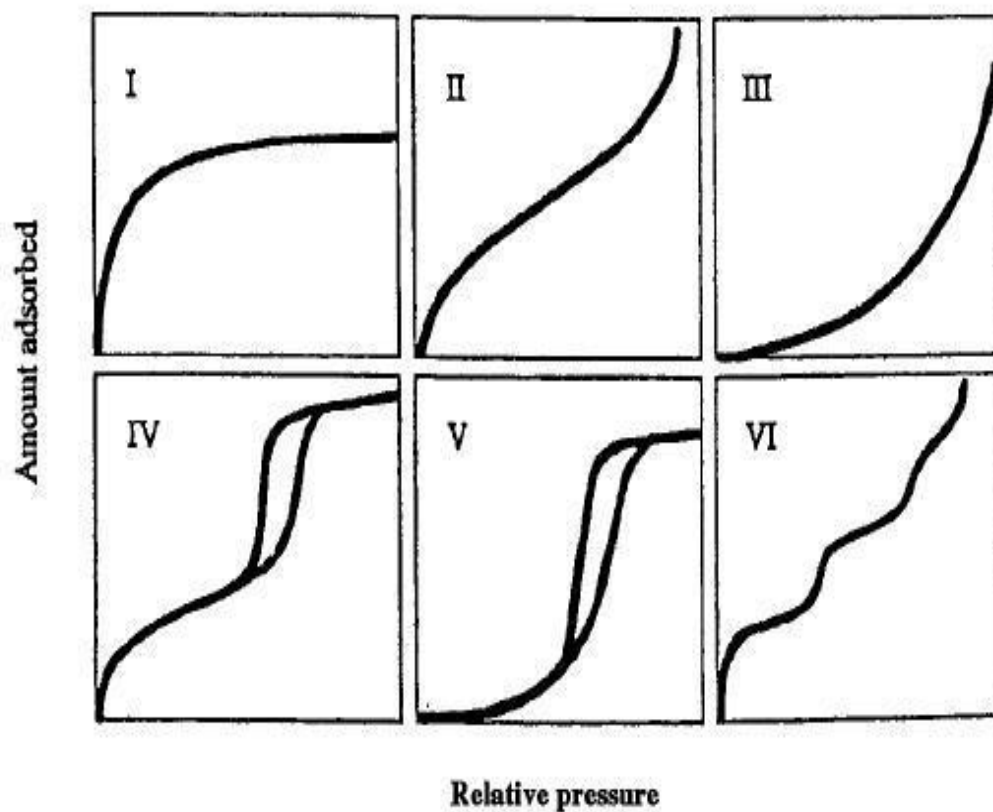
Figure 1.5 The IUPAC Classification for adsorption isotherms [20]

6

1.4 Applications of MCM-41

1.4.1 Heterogeneous catalyst and catalyst support.

Stringent environmental regulations, increasing public concerns, and legislation governing the disposal of hazardous wastes have become a central theme of the modern chemical industry. There are increasing restrictions on the use of traditional stoichiometric and conventional homogeneous catalytic processes because of their inherent problems such as cost, separation, handling and waste disposal. This has accelerated the tendency to shift toward more viable alternatives such as heterogeneous catalysis, which offers the advantages of simple separation and easy recovery, reuse, waste reduction, and elimination of hazardous chemicals, in addition to their use in both liquid- and gas–phase operations. The development of eco-friendly, environmentally compatible, and recyclable solid (heterogeneous) catalysts for the production of fine chemicals and the synthesis of building blocks for pharmaceuticals and agrochemicals is becoming an area of growing interest [21]. MCM-41 is considered promising for a variety of catalytic applications including photocatalysis and enzyme catalysis [22-27]. Silicious MCM-41´s possesses a neutral framework, which limits their applications in catalysis, but they have great utility as adsorbents, molecular sieves, and supports.

1.4.2 Adsorption and Separation Processes

The large pore volume, pore size flexibility, and structural diversity of MCM-41 can be widely exploited for the selective adsorption of a variety of gases, liquids, and solids. Extensive work has been undertaken on sorption properties of several adsorbates, e.g.,

nitrogen, argon, oxygen, water, benzene, toluene, as well as certain lower hydrocarbons and alcohols on MCM-41 [28-34]. It was also demonstrated that the adsorptive capacity of the mesoporous materials is more that an order of magnitude higher than that of conventional sorbents [28-34]. MCM-41 is therefore promising, as a selective adsorbents in separation techniques, e.g., high-performance liquid chromatography and supercritical fluid chromatography [35-37]. Furthermore, the replacement of the surface hydroxyl groups in the pore wall with trimethylsilyl groups creates a more hydrophobic environment that substantially reduces the sorption capacity of polar molecules. Interestingly, MCM-41 offers a method for the recovery of some heavy metal ions such as mercury, lead, and silver from liquid pollutants. For example, grafting of thiol-functionalized tris-(methoxy/propoxy)-mercaptopropylsilane on MCM-41 has shown a remarkable ability to sop up heavy metal ions from wastewater, thus opening a viable route for related environmental and industrial pollution control processes [38- 42].

1.4.3 Molecular Host

The area of quantum structures in confined environments provides several potential applications [43, 44]. In this regard, MCM-41 is promising as a host material because of its mesopore structure. Thus, it is considered as an ideal candidate for the loading and encapsulation of various metals, metal oxides, semiconductor cluster, and nanowires [43, 45-47].

1.5 Aim of this study

The aim of this study is to investigate the sorption equilibrium of C_8 aromatics (p-xylene, m-xylene, o-xylene, and ethylbenzene) on MCM-41 at different temperatures (30°C, 50°C, 65°C, 80°C) considering the vapour pressure data of them by using an automated gravimetric electrobalance system (IGA system).

CHAPTER 2

LITERATURE SURVEY

2.1 History of mesoporous materials

A continuous research in developing materials with constantly larger pores finally led to the development of materials with mesopores (pores between 2-50 nm). The syntheses of these new mesoporous materials were first achieved by Exxonmobil researchers in 1992 [48-53]. These materials were classified according to their different structures as belonging to the "M41S" class materials. These structures were purely siliceous materials. In order to obtain comparable structures with zeolites, the first successful attempts of aluminium incorporation into the framework of these structures were published [54].

The remarkable features of MCM-41 materials include a narrow pore size distribution, high surface area, high pore volume, and high thermal and hydrothermal stability, as well as parallel hexagonal arrays of pores with uniform sizes without pore channel intersection [55-58]. These well-defined structural characteristics make them ideal media to study the adsorption, catalysis, ion exchange, and separation.

Branton et al. studied the adsorption isotherm of argon, nitrogen, and oxygen on MCM-41 sample (surface area 655 m^2/g and effective pore diameter in the range 3.3 -4.3 nm). They showed all the isotherms are type IV in the IUPAC classification. The argon and oxygen isotherms exhibit well defined hysteresis loops and are of a type generally found with well defined mesoporous adsorbents, whereas the nitrogen isotherm is completely reversible. They tentatively concluded that the absence of hysteresis is due to the particular pore shape and size distribution, which results in capillary condensation/evaporation taking place reversibly in the region over P/Po = 0.41 [30].

Branton et al. studied the adsorption isotherms of methanol, ethanol, propan-1-ol, butan-1-ol, and water vapour on MCM-41 sample, a model mesoporous adsorbent at different temperatures (290K, 298K, and 303K). They showed isotherms of alcohols are all type IV, whereas the water isotherm is of type V in the IUPAC classification. Each adsorption isotherm exhibits a sharp step, indicative of capillary condensation within narrow distribution of mesopores. The isotherms are reversible in the monolayer-multilayer region, but distinctive hysteresis loops are associated with the condensation- evaporation cycle. The area within the loop is dependent on the adsorptive, increasing in scale from methanol to butan-1-ol and water. It is evident for the large internal surface of MCM-41 is somewhat hydrophopic and that its mesopore structure is remarkably uniform and stable [31].

Choma et al. studied the benzene adsorption isotherms on three MCM-41 samples and their use for pore size analysis; they focused in this work on the elaboration of methodology for adsorption characterization of porous silicas by using benzene adsorption isotherms. Three MCM-41 samples were synthesized by using (TEOS) as silica source and surfactants, C8, C10, C16, as templates. The samples were characterized by XRD which indicated a good quality of the samples studied.

Benzene adsorption isotherms measured on these MCM-41 samples, were used to evaluate standard quantities such as, the BET specific surface area, total pore volume, external surface area and the volume of ordered mesopores, and to obtain the statistical film thickness as well as the Kelvin-type relation, which describes the dependence between pore width and condensation pressure for benzene on silica at 298K [32]. They compared the results obtained from benzene adsorption isotherms with the result obtained from argon adsorption isotherms at 77K on MCM-41 samples. The results are summarized in Table 2.1 [59].

Table 2.1.Comparison of the parameters obtained from analysis of adsorption isotherms for benzene at 298K and argon at 77K measured on the MCM-41 samples studied [59].

Surfactant used	Adsorbate	S_{BET} (m^2/g)	V_P (cm^3/g)
C_8	Benzene	500	0.43
	Argon	568	0.40
C_{10}	Benzene	720	0.42
	Argon	733	0.51
C_{16}	Benzene	465	0.76
	Argon	600	0.78

As seen in table 2.1 they evaluate the BET surface areas by using benzene adsorption isotherms on MCM-41 samples and compared with the results from argon adsorption isotherms at 77K. The single-point pore volume obtained from benzene adsorption isotherm was obtained by converting the amount of adsorbed benzene at relative pressure about 0.98 and using the molar volume of benzene at 298K, 89.38 cm^3/mol. The V$_P$ obtained was compared with the results from argon adsorption isotherms. From Table 2.1 the V$_P$ increased as the surfactant chain length increased. The statistical film thickness for benzene on the silica surface was calculated by using the Broekhoff and de Boer theory. It was shown that an additional constant correction needs to be introduced to the Kelvin equation (equation 2.1) [1] to extend its applicability to the range of small mesoporous. This correction $\xi = 0.25$ (where ξ is the empirical correction) was found by comparing the pore size distributions from benzene adsorption isotherms with those from argon adsorption isotherms.

$$\mathrm{Ln}\ p/po = -\ \frac{2\gamma V}{rRT}\cos\ \phi \ \dots\dots\dots\dots\dots\dots\dots\dots\dots\dots(2.1)$$

Here po is the saturated vapour pressure at the temperature, T(°K), of the system; γ and V are the surface tension and the molar volume of the adsorbate in liquid form; R is the gas constant per mole and ϕ is the angle of contact between the liquid and the wall of the pore.

Russo et al. studied adsorption of toluene, methylcyclohexane, and neopentane on silica MCM-41. They investigated the effect of temperature on the adsorption isotherms and on the capillary condensation / evaporation processes of toluene, methycyclohexane, and neopentane on MCM-41 material of pore size ~3.4 nm.

The adsorption isotherms of toluene and neopentane were found to be type IV, similar to that of nitrogen but those of methylcyclohexane did not show a knee at low P/Po, indicating weak adsorbate-adsorbent interactions. They found that neopentane adsorbs reversibly in the range of temperatures studied (258 to 278K). On the other hand, at the lowest temperatures the isotherms of toluene and methylcyclohexane exhibited a hysteresis cycle. They found that these two organic adsorbents have very close hysteresis critical temperatures (between 268 and 273K), although the stepwise capillary condensation occurs at different P/Po on pores of the size analysed. They determined the isosteric heats of adsorption from the isotherms at the various temperatures. The three organic adsorptives interact differently with silica surface and the isosteric heats of adsorption indicated that methylcyclohexane has the weakest interaction and toluene the strongest [60].

Mangrulkar et al. studied adsorption of phenol and o-chlorophenol on mesoporous MCM-41 material. They investigated the effect of surfactant template in MCM-41 and calcination on the removal of phenol and o-chlorophenol. It was found that uncalcined MCM-41 shows significant adsorption for phenol and o-chlorophenol as compared to calcined MCM-41. This may be because of the hydrophobicity created by surfactant template in the MCM-41. Batch adsorption studies were carried out to study the effect of various parameters, like adsorbent dose, pH, initial concentration and the presence of co-existing ions.

It was found that adsorption of phenol and o-chlorophenol depends upon the solution pH as well as co-existing ions present in the aqueous solution. The equilibrium adsorption data for phenol and o-chlorophenol was analyzed by using Freundlich adsorption isotherm

model. From the sorption studies it was observed that the uptake of o-chlorophenol was higher than phenol [61].

Qin et al. investigated adsorption of nitrobenzene on MCM-41 from aqueous solution by using batch experiments. Results indicated that nitrobenzene adsorption is initially rapid and the adsorption process reaches a steady state after 1 min.. The adsorption isotherms are well described by Langmuir and Freundlich models, the former being found to provide the better fit with the experimental data. The effect of temperature, pH, ionic strength, humic acid, and the presence of solvent on adsorption processes were examined. It was shown that, the amount of nitrobenzene adsorbed decreases with an increase of temperature, pH, and ionic strength. However, the amount of nitrobenzene adsorbed onto MCM-41 does not show a notable difference in the presence of humic acid. The presence of organic solvent results in a decrease in nitrobenzene adsorption [62].

Monash et al. studied the adsorption of organic dye (methylene blue) on MCM-41 to examine the potential of MCM-41 for the removal of dyes from aqueous solution. The adsorption of methylene blue on MCM-41 with respect to contact time, pH, and temperature was measured to provide more information about the adsorption characteristics of MCM-41. Both Langmuir and Freundlich adsorption models were applied to describe the equilibrium isotherms. MCM-41 sample was synthesized and characterized based on the analysis of the nitrogen adsorption/desorption isotherms, XRD patterns, and thermo gravimetric analysis (TGA) [63].

CHAPTER 3

EXPERIMENTAL

3.1 Synthesis of MCM-41

MCM-41sample was synthesized in Chemical Engineering Department of Gazi University by Ms. Arzu Solmaz as summarized below [70].

3.1.1 Synthesis work

Synthesis of MCM-41 was done by direct hydrothermal synthesis method. The materials used in MCM-41 synthesis were basically silica source, surfactant, and solvents. Starting from the formula that was determined by Güçbilmez [16], the molar amounts of the substances that were used for MCM-41 synthesis were calculated. The ratio between these substances were found as, 0.51 mol surfactant cetyltrimethylammoniumbromides (CTMABr) and 55 mol water (H_2O) for one mol of silica (SiO_2). By using these ratios; the details to synthesis MCM-41 to obtain 100g synthesis solution approximately, were given below.

1. 13.2 g surfactant (CTMABr) and 70 ml deionized water were mixed with a magnetic stirrer with heating to prepare surfactant solution. Temperature of solvent was kept at constant 28°C.

2. The surfactant solution was added drop by drop into 11.3 ml (15.7 g) sodium silicate composition and this solution was mixed by magnetic stirrer until a gel forms.

3. pH of the gel formed at the second step was adjusted to 11.0 by 4N H_2SO_4 solution.

4. For the formation of MCM-41 crystals, gel whose pH was adjusted was placed into an autoclave that had a Teflon plate in it and has a stainless steel outer surface. Gel was hold at 120°C for 96 hours (4 days).

5. The mixture that removed from autoclave was filtrated to remove the solid phase from the gel. Obtained solid material was washed by deionized water with a vacuum filtration system until its pH reached to a value of 7.0.

6. Dried solid product was placed into quartz reactor that has membrane filter in the middle of it, and reactor was placed into a horizontal tubular furnace. A continuous dry air flow was supplied on the reactor (reactor radius was 1.5 cm and the length was 100cm). The temperature of the tubular furnace was raised to 550°C starting from room temperature with heating ramp rate of 1°C/ min. and solid sample was calcinated by holding it at 550°C for 6 hours.

3.2 Materials and Apparatus for Sorption Measurement

IGA system was used to investigate the sorption equilibrium of C_8 aromatics (p-xylene, m-xylene, o-xylene, and ethylbenzene) on MCM-41 at different temperatures (30°C, 50°C, 65°C, 80°C).

3.2.1 Apparatus

The model IGA-002 system consists of computer-controlled microbalance system, stainless steel reactor, adsorbate reservoir, vacuum station, standard furnace, anti-condensation system and an automated and manual valve. The apparatus is shown in Figure 3.1.
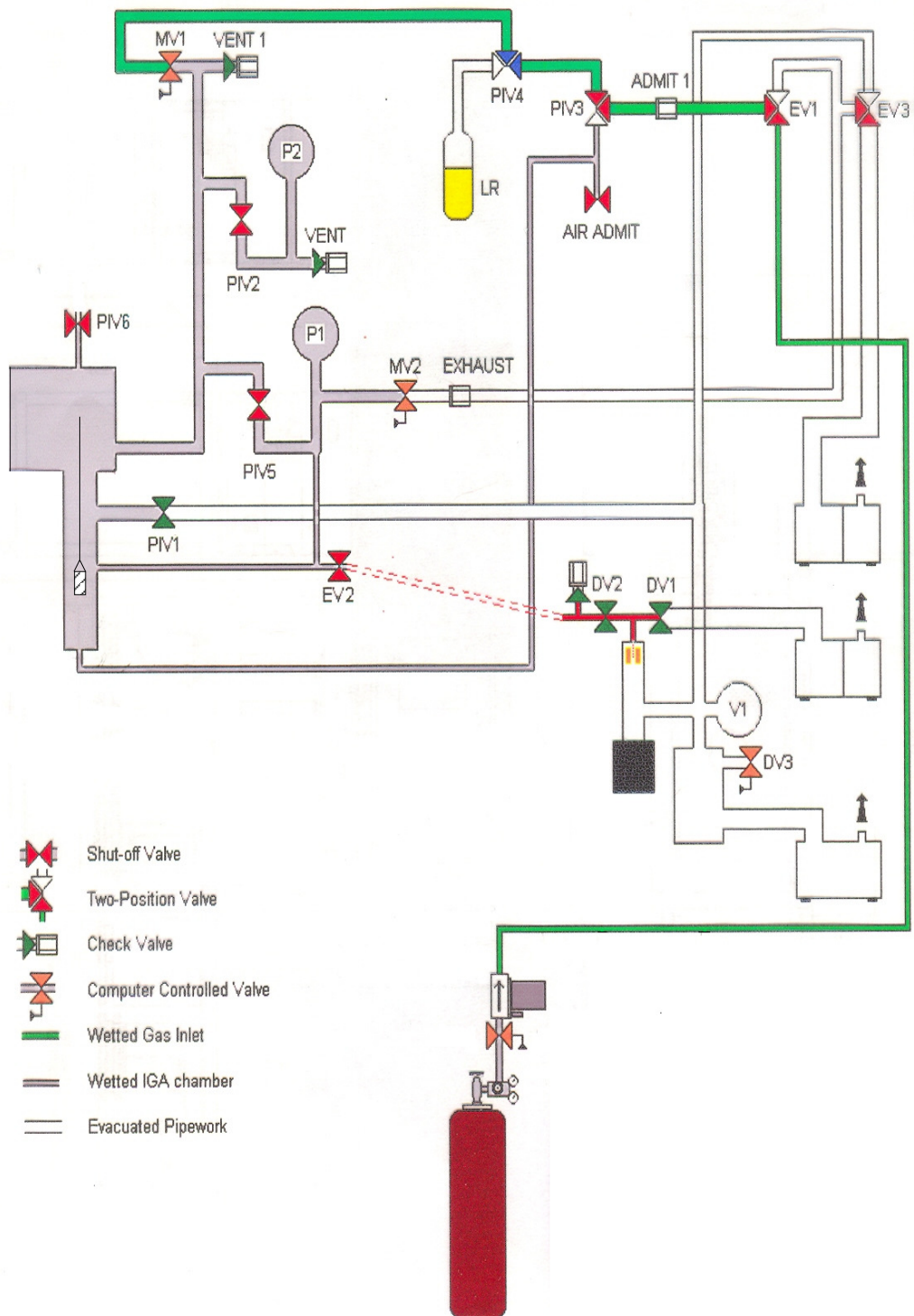
Figure 3.1, IGA-002 configuration set for static gas operation (Idle mode)

The microbalance system that contained the MCM-41 sample container (pan) forms the core of the IGA range of gravimetric analysers. The IGA design integrates precise computer-control and measurement of weight change, pressure and temperature to enable fully automatic and reproducible determination of sorption isotherms. The vacuum systems for de-pressurisation and outgassing are offered to two levels of vacuum. Rotary pump station for operation to 10^{-2} mbar, comprising of two-stage rotary pump. High vacuum turbomolecular pump station for operation to 10^{-6} mbar. Standard furnace for sample outgassing to 500°C and set-point regulation (isotherm temperature) between 20°C-500°C. The protection against condensation is generally referred to 'Anti-condensation protection part' and this part operates in conjunctions with thermostats and temperature sensors to define and measure the temperature of the champer.

3.2.2 Sorbates

The sorbates were used without any purification step and their grades and sources are given in Table 3.1.

Table 3.1 Grades and origins of sorbates.

Sorbate	Grade	Supplier
p-xylene	Chemically pure	Fluka
m-xylene	Chemically pure	Fluka
o-xylene	Chemically pure	Fluka
Ethylbenzene	Chemically pure	Fluka

Critical temperatures and vapour pressures at (30°C, 50°C, 65°C, 80°C) of sorbates are given in Table C.2 in Appendix C.

3.2.3 Experimental procedure

The adsorption isotherms of p-xylene, m-xylene, o-xylene, and ethylbenzene have been determined by using an automated gravimetric electrobalance system (IGA-002 system, HIDEN), (Appendix D). By following the main steps illustrated below.

```
┌──────────────────────┐        ┌──────────────────────┐
│  Loading MCM-41       │        │  Loading the sorbate  │
│  sample and make the  │───────▶│  and make             │
│  first regeneration   │        │  decontamination      │
└──────────────────────┘        └──────────────────────┘
                                            │
                                            ▼
┌──────────────────────┐        ┌──────────────────────┐
│  Regeneration         │        │  Setup the temperature│
│                       │───────▶│  of Anti-condensation │
└──────────────────────┘        │  protection system    │
         ▲                       └──────────────────────┘
┌──────────────────────┐                    │
│  Plot isotherm data   │                    ▼
└──────────────────────┘        ┌──────────────────────┐
         ▲                       │  Setup the            │
┌──────────────────────┐        │  temperature of       │
│  Setup the pressure   │◀───────│  isotherm             │
│  points for adsorption│        └──────────────────────┘
│  isotherm             │
└──────────────────────┘
```
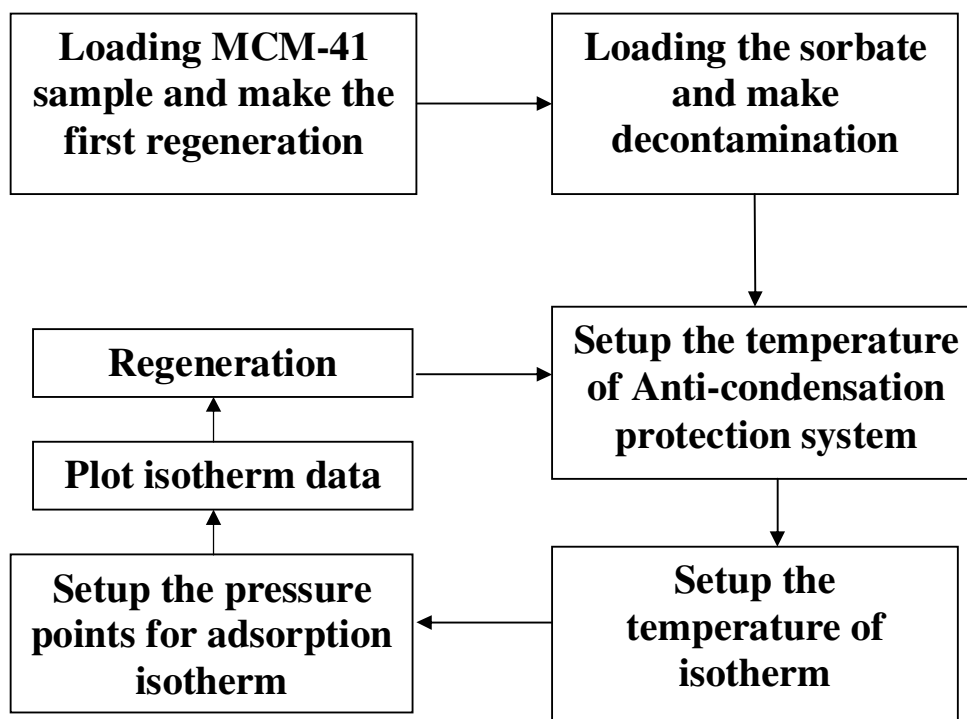
Figure 3.2, Experimental procedures steps

3.2.3.1 Loading MCM-41 sample

IGA software guides us through the procedure for sample loading. This selection is not possible unless the old sample is unloaded. This means that we must first execute the unloading procedure [64]. We must be sure that the pressure and temperature control are inactive, and we should let the air enter to the reactor before we start loading the sample. Sample loading is straightforward if we use the same type of sample container with approximately the same sample size each time, by lowering the sample reactor whilst supporting the reactor tube, for example using the 'claw' finger position shown below. To ensure that the reactor is kept upright whilst lowering until it is clear of the sample position.

Figure 3.3, lowering the sample reactor

The sample container (pan) should be removed using the container carrier and either cleaned and replaced or a substitute container replaced on the balance. Then remove the old container and gently attach the new one with MCM-41 sample using the container carrier and replace the reactor tube as a draught shield.
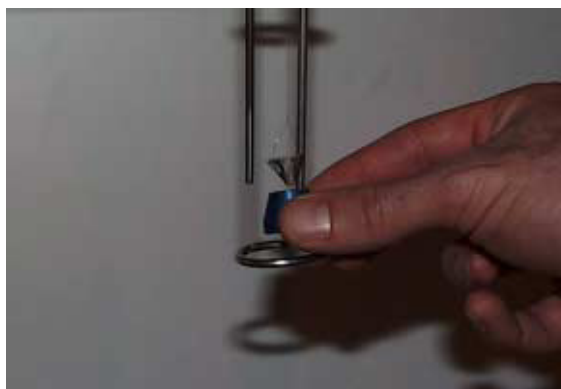
Figure 3.4, Loading sample container (pan)

Each new sample is given an incremental identification sample number between 2 and 9999. The sample number is ultimately displayed at the top of the screen together with a title. The combination of number and title are used to identify the experiments. After loading the sample we can start the experiments.

3.2.3.2 Loading the sorbate

To load the sorbate we should follow this:

1- Remove the front access cover of the IGA.

2- Rotate PIV4 so that it is in the upward position.

3- Remove the stainless steel reservoir by loosening off the VCR holding nut with a " ¾ " spanner.

4- Empty, clean, and bake out the reservoir, or replace with alternate reservoir.

5- Remove the used VCR-4 gasket and replace with a new gasket. Never tighten the VCR holding nut without a gasket in place.

6- Move the reservoir back into position, and retighten the VCR holding nut.

If the sorbate is to be changed, we will first need to decontaminate the vapour delivery pipework.

3.2.3.2.1. Decontamination

The term decontamination for the IGA applies to removing impurities from the gas or vapour connection to the system, i.e., from the supply connection to MV1 (Figure. 3.1). There will generally be air (including water vapour) when the sorbate reservoir is changed. We must be ensure at this point that PIV1 valve at the bottom (green valve) of the IGA is closed, and pressure control is inactive (the 'p' led on the front panel of the IGA should be extinguished). First we should connect the empty reservoir, then we should slowly rotate PIV4 left, then we should select 'decontamination' from pressure set window. At this point we need the current password. The admittance valve (i.e., MV1) will open fully. Then by degassing the reactor by execute '**Outgas'**, from pressure control window with a ramp rate (100 mbar/min is typical but more caution is required with fine powder (such as our sample), 10 mbar/min is recommended). As the admit valve is fully open, the vapour admit pipework will be decontaminated as the entire system is evacuated. We will wait until the PIV1 button in pressure set window is active ('LED' stays illuminated). Then we select PIV1 button from pressure set window and slowly open it (PIV1 valve beneath the IGA cabinet).

3.2.3.3 Setup the temperature of Anti-condensation protection system

The temperature of "Anti-condensation protection system" in the IGA, "ACS temperature" was specified as (50°C) for all experiments.

3.2.3.4 Setup the temperature of isotherm

The temperature control parameters and options are set or changed in the temperature set window:
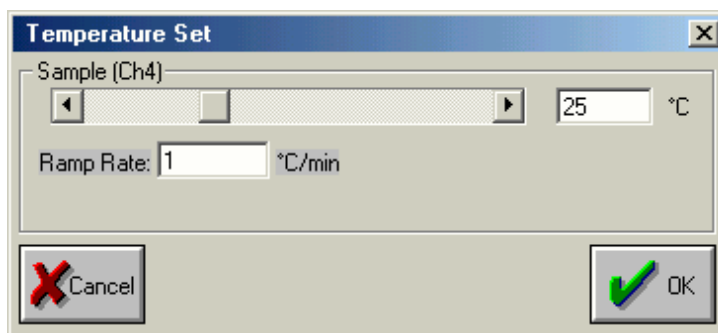
Figure 3.5, Temperature setup window

The set- point can be changed using the mouse to drag or activate direction controls for the slider or by direct edit of the displayed temperature so we can setup the furnace temperature (i.e., isotherm temperature). This displayed value will be subsequently reset to the nearest value equivalent to the digital resolution of measured temperature. Ramp rate with in allowed control limits can be entered.

3.2.3.5 Setup the pressure points for adsorption isotherm.

The sorption/desorption set-points were entered in the category of the isotherms setup window:
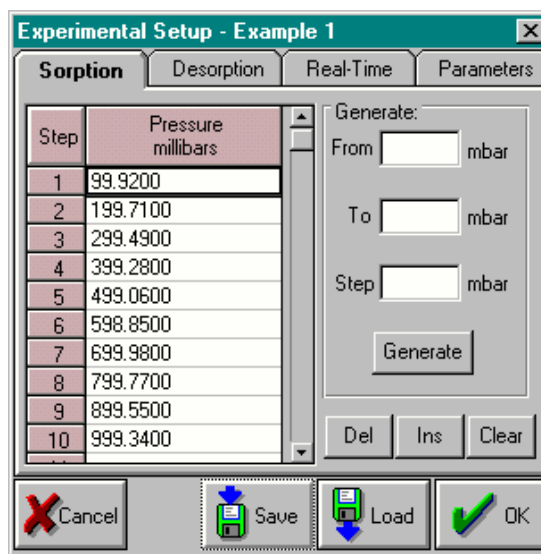
Figure 3.6, Isotherm setup window

The sorption set-points must be increasing pressure values in the grid order (according to the saturated vapour pressure of the sorbate at the isotherm temperature), desorption set-points must be decreasing pressure values in the grid order, blanks are not allowed and the pressure change must be at or above the minimum control increment (equivalent to ~ 0.05% of the pressure range). In addition, during the experiment, the pressure values may not exactly correspond with the grid. The reason is that, for example, on adsorption the software checks the grid for the next highest pressure above the minimum control increment. This means that we can start the isotherm with any initial pressure in the chamber and on adsorption the first isotherm point will be the next highest grid value for which the pressure change is above the minimum increment.

3.2.3.6 Plot isotherm data

Equilibrium data (for selected x, y1-or y2- axis fields) were plotted by the selection of, **Replay Isotherm** tool**,** from tool Bar in the IGA software window. The sample (run) number is selected from drop-down file select list at the top of the window and then the required isotherm scans were selected too in the plot column and then the graph produced. The isotherm is typically plotted as x-field = P/Po and y-field= % mass.

3.2.3.7 Regeneration

Regeneration for MCM-41 sample was needed after every sorption experiment. The regeneration started by rotating PIV4 to be in vertical position (close position) then by degassing the reactor by execution '**Outgas'**, from pressure control. De-pressurisation is achieved by the computer controlled valve MV2 which will open to the vacuum pump. One special condition here is complete de-pressurisation to base vacuum which is called **'Outgas'** (vacuum drying) where ultimately MV2 fully opens and entire chamber was evacuated. Then heating the MCM-41 sample up to 200°C with ramp rate (5°C/min) under high vacuum (10^{-6} mbars) we reach it by using high vacuum turbomolecular pump for four hours. The high conductance exhaust valve PIV1 was also gently opened at this stage to improve the efficiency of evacuation and the control PIV1 must be selected in the pressure set window. After four hours MCM-41 sample, will be cooled to the next isotherm experiment temperature by stop heating via execute "stop" button from temperature set window. After closing the high conductance exhaust valve PIV1 and then turn off turbomolecular pump. Then start the next isotherm experiment.

CHAPTER 4

RESULTS AND DISCUSSIONS

In this chapter the characterization of MCM-41 sample by XRD and nitrogen physisorption analysis are presented. The sorption capacities of C_8 aromatics (p-xylene, m-xylene, o-xylene, and ethylbenzene) on MCM-41 are obtained by using IGA system and presented in Tables (B.1-B.44) and Figures (4.6-4.20).

The sorption isotherms for p-xylene, m-xylene, o-xylene, and ethylbenzene on MCM-41 were measured at different temperatures (30°C, 50°C, 65°C, and 80°C). During the sorption experiments, initial pressure was usually around 10^{-6} milibars, and final pressures change between (11.13– 41.97 milibars) depending on the vapour pressure of the sorbates at 50°C, which is the maximum temperature of 'Anti-condensation protection' part in IGA system. The pressure of sorbate should be kept below the vapour pressures of adsorbates at 50°C to prevent condensation in this chamber. The vapour pressure of adsorbates was calculated by Antoine equation (Appendix C)

4.1 Characterization of MCM-41

MCM-41 sample was characterized by XRD, and nitrogen physisorption analysis.

4.1.1 X-Ray Diffraction (XRD) Analysis

The XRD pattern of MCM-41 sample is given in Figure 4.1 was performed by Rigaku Ultima IV in-plane diffractometer with X-ray source Cu Kα in central laboratory at METU. It is seen that, the characteristic peak in the low-angle region corresponding to $2\theta = 2.406°$ was obtained for MCM-41.

A typical MCM-41 material synthesized should have three reflections corresponding to 2θ values of around $2.49°$, $4.27°$, and $4.93°$. A fourth peak corresponding to $6.50°$ may sometimes be present. If the synthesized material is of high quality a fifth peak corresponding to $7.35°$ may also be present [66].

The 2θ value ($2\theta = 2.406°$) obtained for the synthesized MCM-41 sample indicates high structural ordering of the MCM-41 sample.
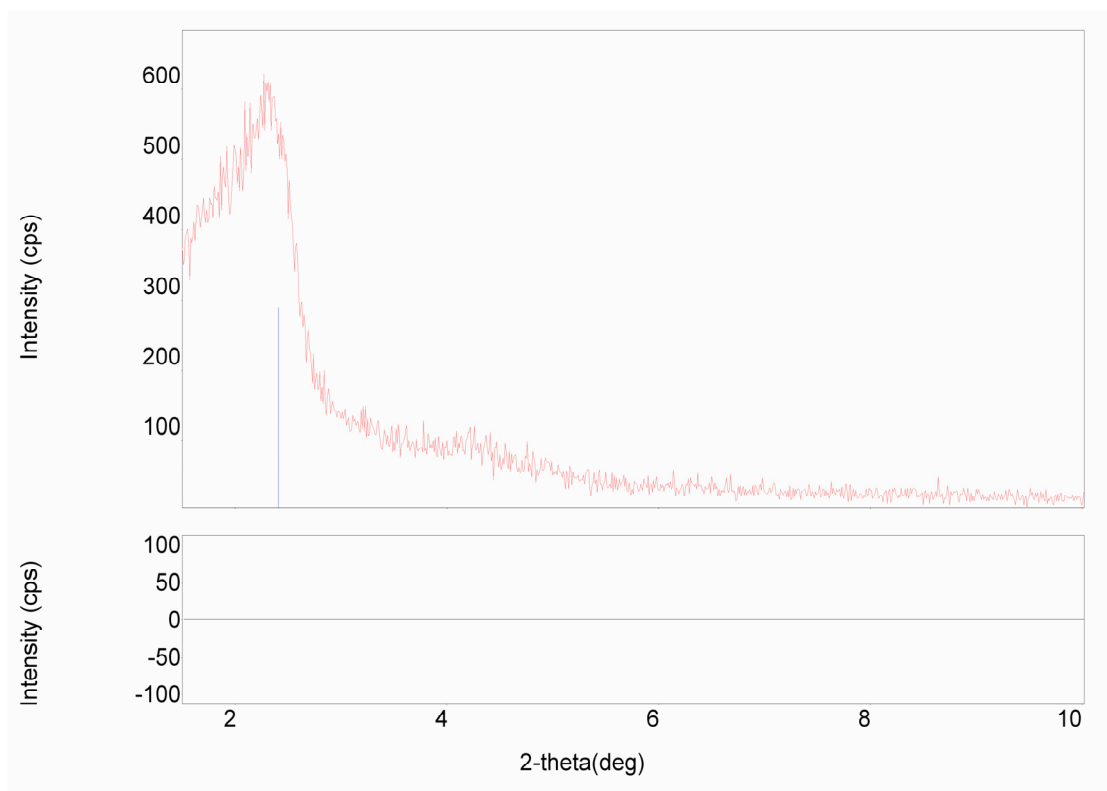
Figure 4.1 XRD pattern of MCM-41

4.1.2 Nitrogen Physisorption Analysis

The BET surface areas, the BJH adsorption pore diameters and the single point total pore volume of the synthesized MCM-41 sample were obtained using their nitrogen adsorption and desorption isotherms. Nitrogen adsorption experiments of MCM-41 sample was performed by Quantachrome Autosorb, Automated Gas Sorption System in Middle East Technical University, Central Laboratory.

The nitrogen adsorption isotherms of the MCM-41 after the 1st and 2nd calcination (where MCM-41 was calcined at 550°C for four hours) showed a typical type V isotherm, as described by the IUPAC classification (Figures A.5, A.6).

BET surface area, pore volume at 0.95 relative pressure, and pore diameter values of MCM-41 sample are listed in Table 4.1. It is clearly seen from Table 4.1 that low surface area for MCM-41 sample compared to other BET surface area values reported in literature, Şener et al. found the BET surface area 999 m^2/g [75] and Branton et al. found BET surface area 655 m^2/g [31], which may be due to the fewer defects in MCM-41 sample [67]. The surface area of MCM-41 depend on the synthesis method and surfactant that was used as template. Choma et al. found BET surface area for MCM-41 sample (465 m^2/g) by using the same synthesized method and the same surfactant [32]. MCM-41 sample have pore size in the mesoporous range. Pore size distribution curves for adsorption for MCM-41 is given in Figure 4.2, 4.3. As shown in the figures, pore size distribution of MCM-41 was very narrow. When we compare BET surface areas after the 1st and 2nd calcination there is not too much difference between them, this show thermal stability of MCM-41 and the high ordering structure of MCM-41 sample.

Table 4.1 Surface areas, pore volume, and BJH adsorption pore diameter of MCM-41 sample

Sample	BET surface area (m^2/g)	pore volume (V_P) at P/Po 0.95(cc/g)	BJH adsorption pore diameter (nm)
MCM-41 after the 1st calcination	474.5	0.50	2.475
MCM-41 after the 2nd calcination	492.2	0.45	2.456
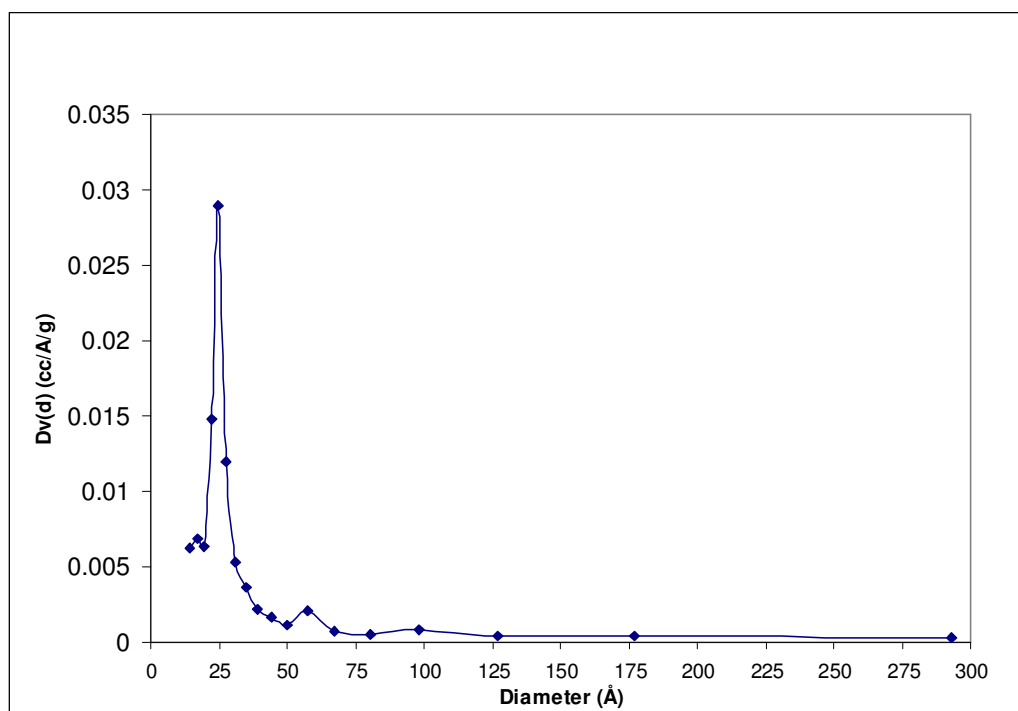
Figure 4.2 BJH adsorption pore size distribution of MCM-41 sample after the 1st calcination.
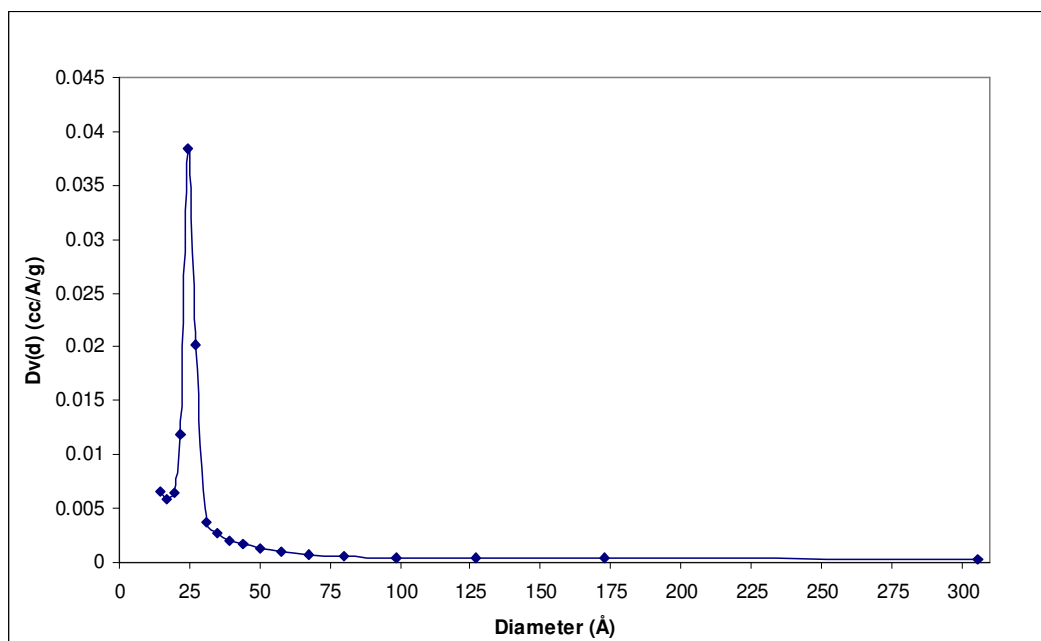
Figure 4.3 BJH adsorption pore size distribution of MCM-41 sample after the 2nd calcination.

4.2 Sorption of p-xylene, m-xylene, and o-xylene on MCM-41

The sorption capacities of p-xylene, m-xylene, and o-xylene on MCM-41 sample (MCM-41 sample with one step calcination was used), the isomers which has the kinetics diameters (5.85Å, 6.2Å, 6.8Å respectively) [4] at different temperatures (30°C, 50°C, 65°C, 80°C) were presented in Figures 4.4- 4.15 and Tables (B.1– B.36).
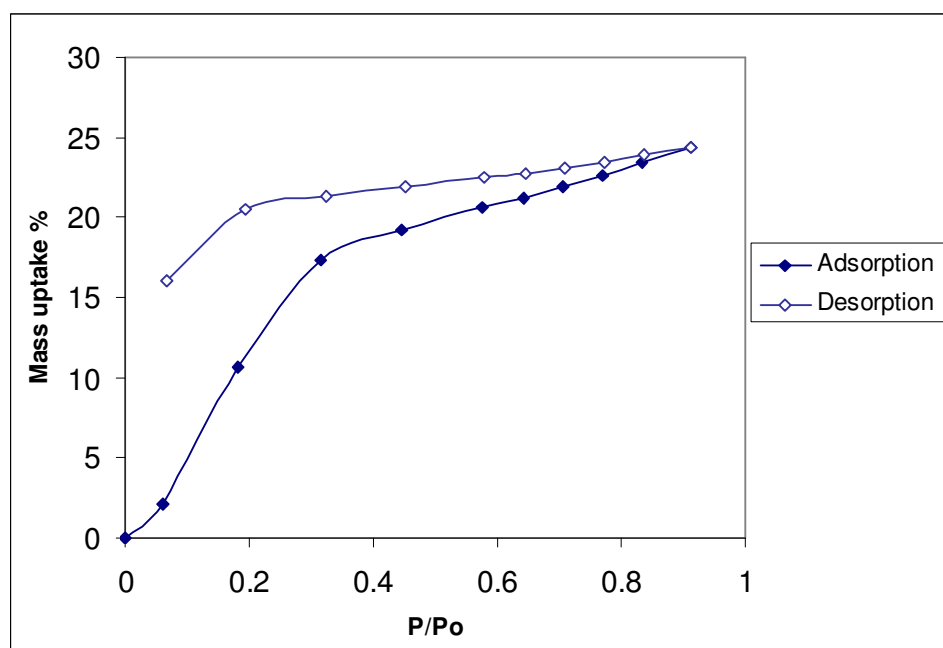
Figure 4.4, Adsorption isotherm of p-xylene on MCM-41 at 30°C.
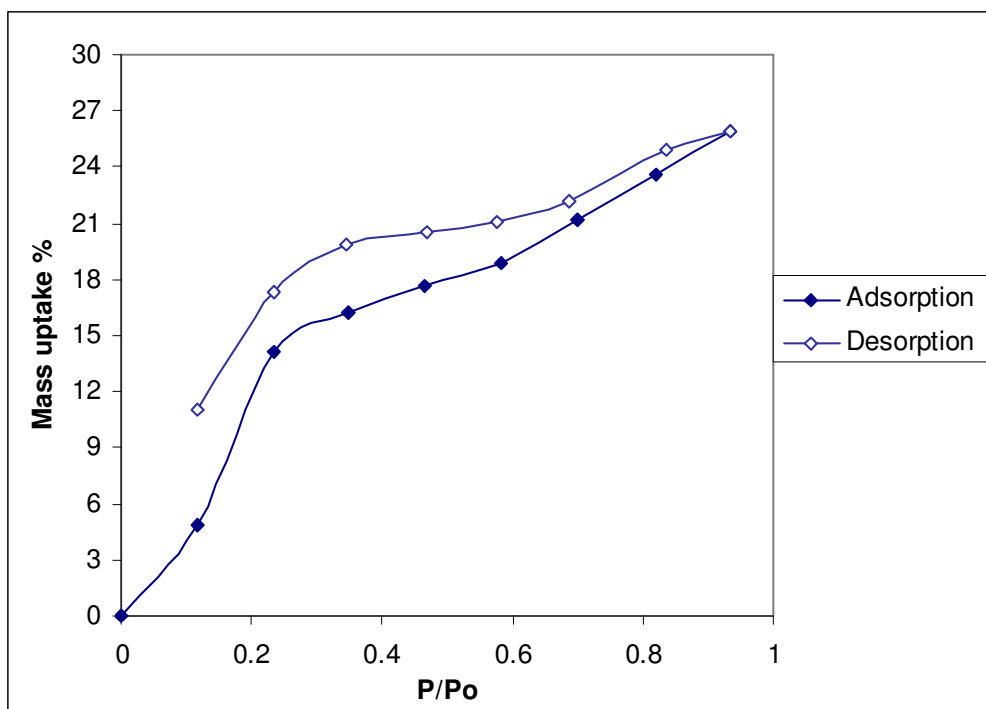
Figure 4.5, Adsorption isotherm of p-xylene on MCM-41 at 50°C.

Figure 4.6, Adsorption isotherm of p-xylene on MCM-41 at 65°C.
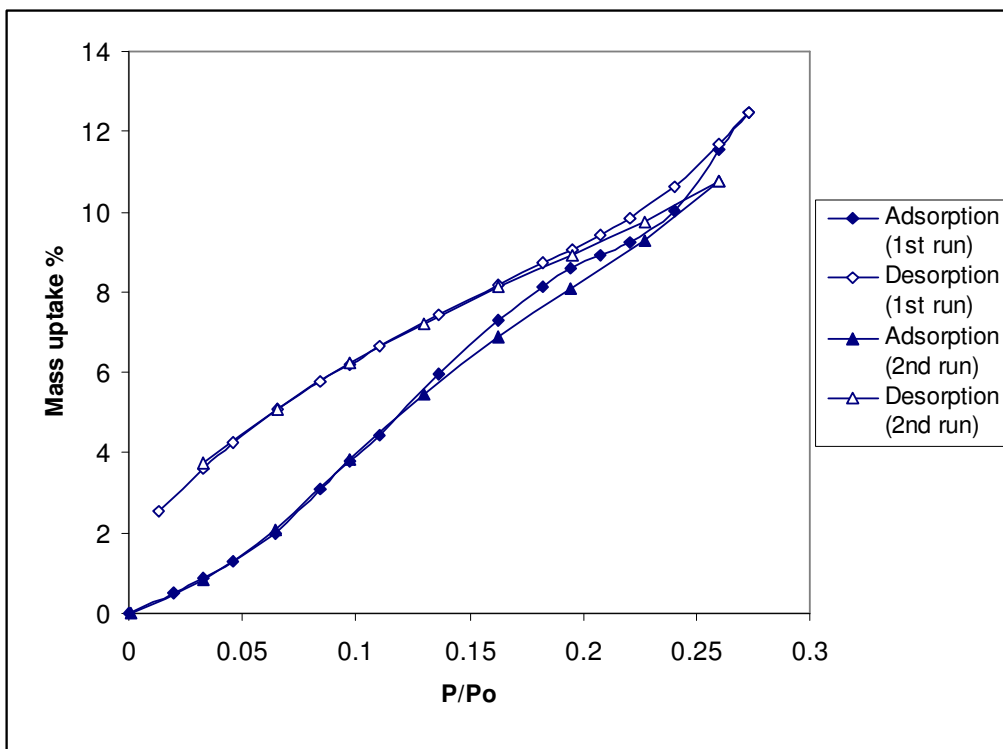
Figure 4.7, Comparison of adsorption isotherms for p-xylene at 80°C

Figure 4.8, Adsorption isotherm of m-xylene on MCM-41 at 30 °C.

Figure 4.9, Adsorption isotherm of m-xylene on MCM-41 at 50 °C.

Figure 4.10, Adsorption isotherm of m-xylene on MCM-41 at 65 °C.
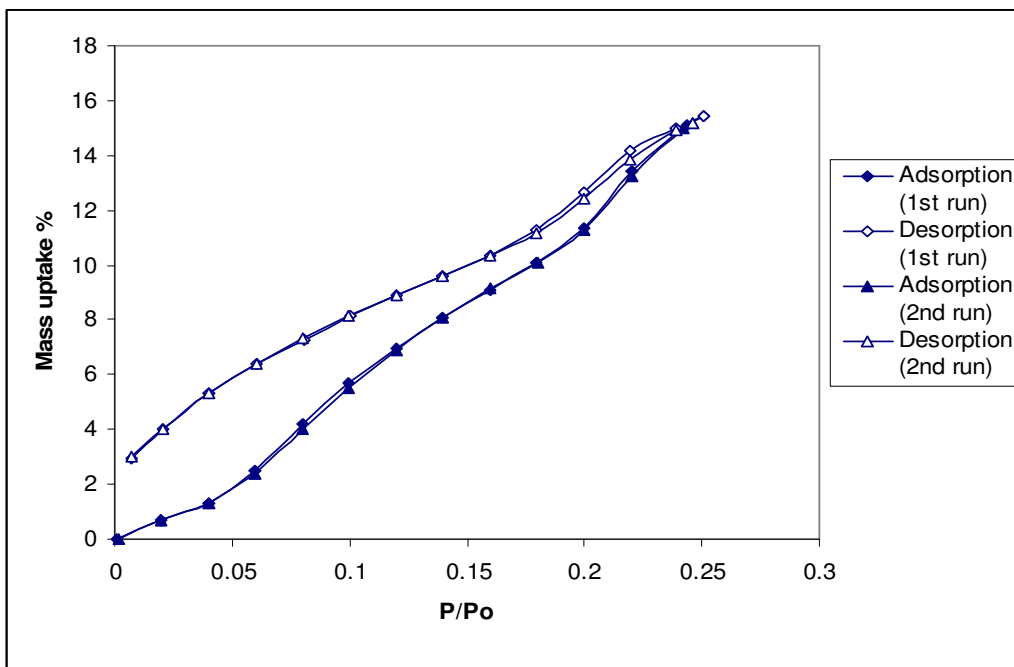
Figure 4.11, Comparison of adsorption isotherms for m-xylene at 80°C

Figure 4.12 Adsorption isotherm of o-xylene on two MCM-41
samples (used and fresh sample) at 30°C.
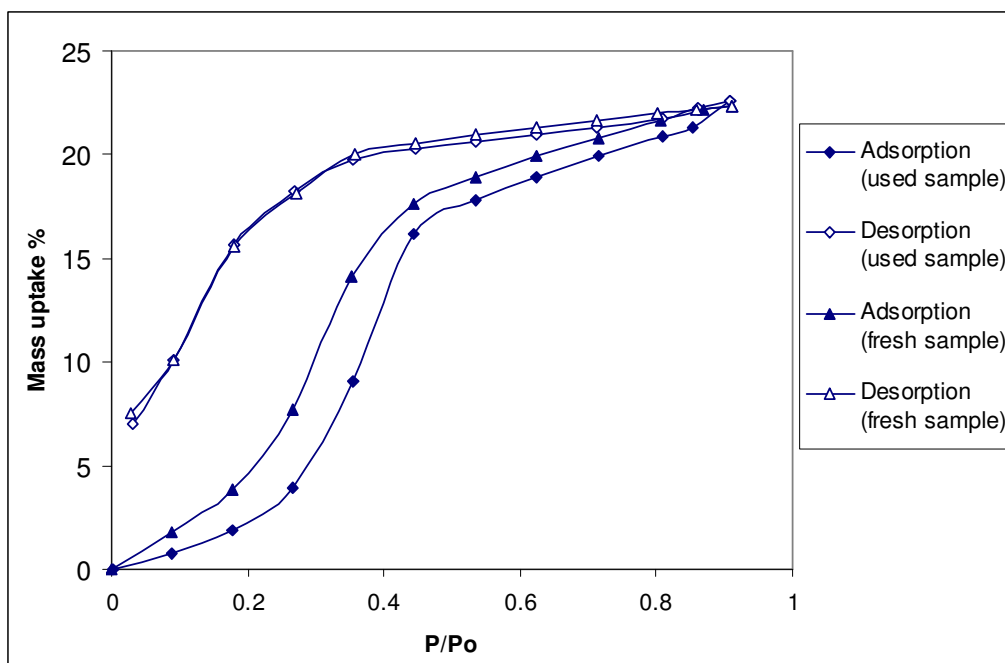
Figure 4.13 Adsorption isotherm of o-xylene on two MCM-41
samples (used and fresh sample) at 50°C.
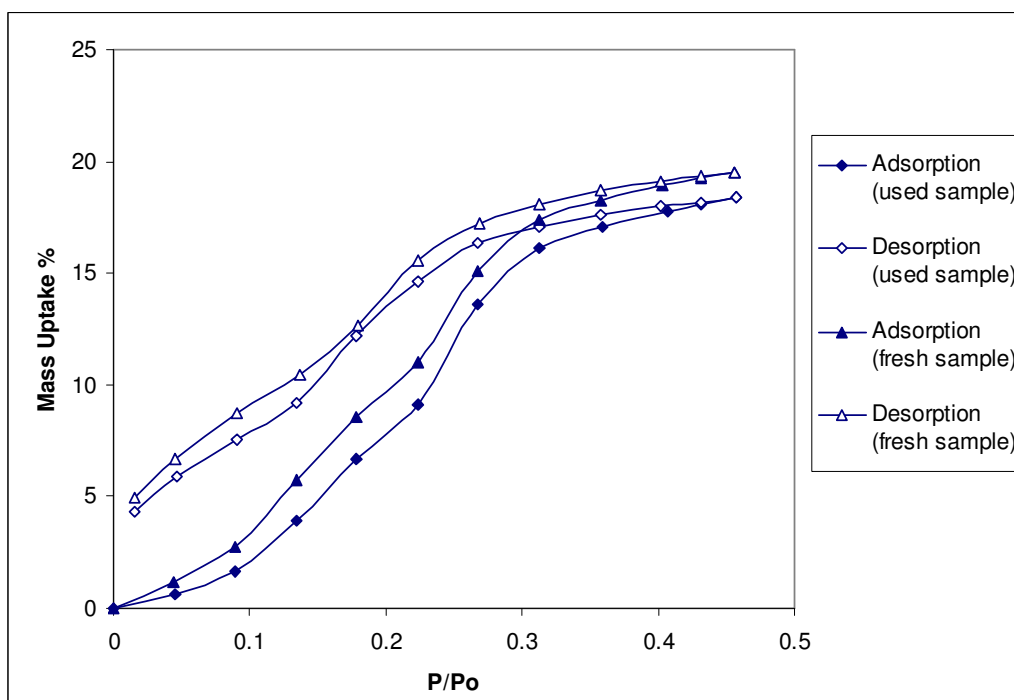
Figure 4.14 Adsorption isotherm of o-xylene on two MCM-41
samples (used and fresh sample) at 65°C.
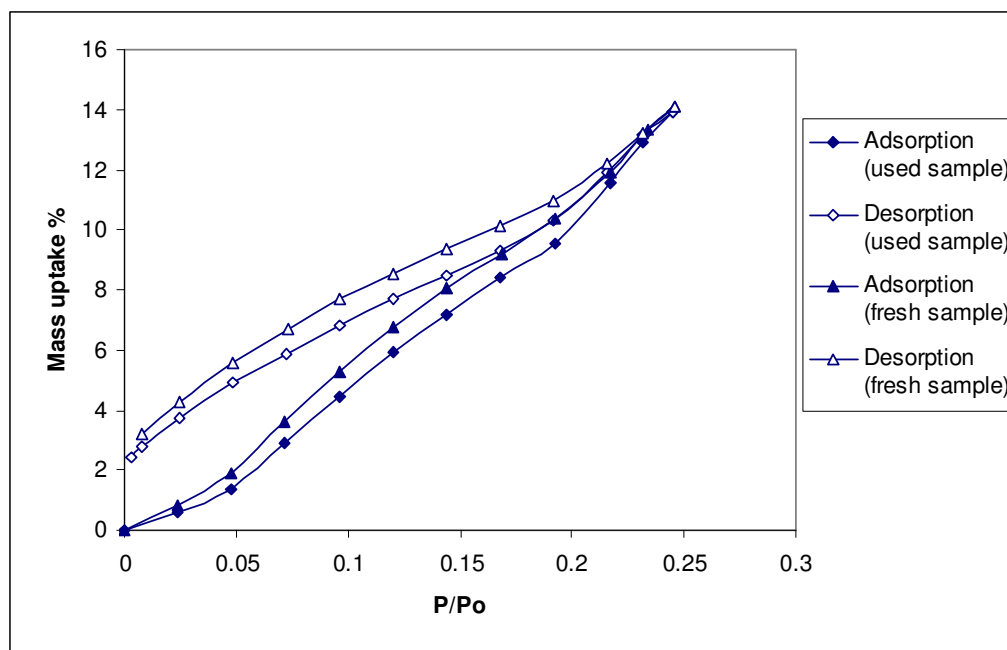
Figure 4.15 Adsorption isotherm of o-xylene on two MCM-41
samples (used and fresh sample) at 80°C.

As seen from Tables (4.2-4.5) and figures (4.4-4.15) we could reach to a
relatively high relative pressure at 30°C and 50°C, while we could not
reach to high relative pressure at 65°C, and 80°C. The reason for this is
that at these temperatures (i.e., 65°C, 80°C) the maximum temperature
of 'Anti-condensation protection' part in IGA system is 50°C, so the
pressure of this chamber (anti-condensation protection part) should be
kept below the vapour pressure of the sorbates at 50°C to prevent
condensation in this chamber.

Table 4.2 Equilibrium sorption capacities for p-xylene.

Temperature (°C)	Maximum pressure(milibars)	Total mass (miligrams)	Maximum relative pressure	Mass uptake %
30	14.1490	25.1042	0.9110	24.4266
50	39.9607	25.4715	0.9334	25.9151
65	41.9260	22.9677	0.4999	17.4740
80	41.9807	21.9203	0.2730	12.4752

Table 4.3 Equilibrium sorption capacities for m-xylene.

Temperature (°C)	Maximum pressure(milibars)	Total mass (miligrams)	Maximum relative pressure	Mass uptake %
30	13.9449	23.9303	0.9266	19.5701
50	36.6234	24.5566	0.8774	21.3085
65	37.6167	23.7920	0.4596	19.1703
80	37.6441	22.9939	0.2506	15.4086

Table 4.4 Equilibrium sorption capacities for o-xylene (used sample).

Temperature (°C)	Maximum pressure(Milibars)	Total mass (miligrams)	Maximum relative pressure	Mass uptake %
30	11.1379	22.6116	0.9434	13.2306
50	30.6099	23.9029	0.9093	22.6022
65	30.6726	22.9809	0.4569	18.3618
80	30.6776	22.0040	0.2454	13.9176

Table 4.5 Equilibrium sorption capacities for o-xylene (fresh sample).

Temperature (°C)	Maximum pressure(Milibars)	Total mass (miligrams)	Maximum relative pressure	Mass uptake %
30	11.1772	25.0552	0.9468	23.9638
50	30.6550	24.7023	0.9107	22.3861
65	30.6258	24.0173	0.4562	19.4944
80	30.6895	22.8914	0.2455	14.1192

The total amounts of all isomers adsorbed at the given pessure on MCM-41 decreased as the temperature of the adsorption isotherms increases (Figures A.1, A.2, A.4 and Tables 4.6, 4.7, 4.8). The decrease of adsorbed amount is due to the decrease of density of the sorbates (p-xylene, m-xylene, and o-xylene) with the increase of adsorption temperature and due to the adsorption equilibrium of the physical adsorption process. Qiao and his co-workers observed similar behavior for hexane adsorption on MCM-41 silica [68]. The repetition of adsorption isotherms at 80°C for p-xylene and m-xylene show the runs are reproducible. For o-xylene the adsorbed amounts was increased by using fresh MCM-41 sample for all the adsorption isotherm experiments at different temperatures due to fresh MCM-41 sample was used.

Table 4.6 Comparison of sorption capacities for p-xylene at same pressure values

Temperature (°C)	pressure(Milibars)	Total mass (miligrams)	Mass uptake %
30	14.1490	25.1042	24.4266
50	14.9618	23.5036	16.1870
65	14.9934	20.7113	5.93310
80	14.9913	20.2282	3.79290

Table 4.7 Comparison of sorption capacities for m-xylene at same pressure values

Temperature (°C)	pressure(Milibars)	Total mass (miligrams)	Mass uptake %
30	11.8847	23.4602	17.2212
50	11.9267	22.1058	9.20160
65	11.9712	21.3143	6.75990
80	11.9919	20.7668	4.23050

Table 4.8 Comparison of sorption capacities for o-xylene (used sample)

at same pressure values

Temperature (°C)	pressure(Milibars)	Total mass (miligrams)	Mass uptake %
30	8.9747	21.8836	9.5851
50	8.9750	20.2682	3.9592
65	9.0080	20.1832	3.9524
80	8.9952	19.8765	2.9033

As seen from the Figures (4.4- 4.15) the adsorption isotherms for all the experiments were found as type V according to IUPAC isotherm classification. Öztin [4] studied sorption of p-xylene, m-xylene, o-xylene, and ethylbenzene on HZSM-35. He found the adsorption isotherms as type I due to the microporous nature of HZSM-35 zeolite.

The capillary condensation-evaporation within a narrow distribution of mesopores was associated with each adsorption isotherm. Condensation takes place in each section at relative pressure provided by the Kelvin equation (equation 2.1)[1], but evaporation from the pore body cannot occur while the pore mouth remains filled.

On the other hand, the meniscus is cylindrical during condensation and hemispherical during evaporation. The desorption occurs via evaporation of the adsorbate from mesopores and usually takes place at a relative pressure lower than that of capillary condensation, resulting in hysteresis loop, which indicate that, the amount of isomers adsorbed being greater at any given relative pressure along the "desorption" branch than along the "adsorption" branch [1]. Hysteresis was shown clearly among all the adsorption isotherm curves. The hysteresis is, in general, attributed to the different sizes of the pore mouths and pore bodies or to the different adsorption and desorption behaviors in near-cylindrical pores. It was

shown that as the temperatures for the adsorption isotherms increases the size of hysteresis decrease.

For many years it has been recognised that the certain forms of physisorption hysteresis are associated with capillary condensation in mesoporous media and that the type of loop is to some extent governed by both the pore shape and the nature of the network [1, 71]. Everett and his co-workers[72], have drawn attention also to the importance of the adsorptive and temperature. They point out that the dependence of the position of the lower limit of the hysteresis loop on pore size and temperature presents a fundamental problem. It now seems likely that, for a given adsoption system, instability of the capillary condensate can arise in at least two ways: either (i) at constant temperature, if the pore dimensions are reduced below the critical level [70], which is not the case in our study, or (ii) at constant pore size, if the temperature is increased sufficiently, which is our case, but for our work the intersection point for the hysteresis loop in the lower limit in the adsorption isotherm curves does not occur.

As seen from Figures (A.1, A.2, A.4) as the temperature of adsorption isotherms increases the values of pressure (or relative pressure for a given adsorption isotherm curve) for the same value of total mass adsorbed of sorbates was increased. Qiao and his co-workers[68] showed that as the temperature increase the capillary condensation steps shift from low to high relative pressures. The large shift of the phase transition from low to high relative pressures originates from the decrease of the surface tension as temperature increase, that is, it needs higher pressure to achieve the capillary adsorption phase transition at the lower surface tension.

The volume of sorbates (V_P) in Tables (4.9-4.11) have been obtained from the amounts adsorbed at different maximum relative pressures by assuming that the pores are filled with condensed sorbate in the normal liquid state.

Table 4.9, The adsorbed volumes (V_P) of p-xylene at different

temperatures and maximum relative pressures.

Temperature (°C)	Maximum relative pressure	Density (g/ cm^3)[73]	V_P (cm^3/g)
30	0.9110	0.8524	0.2865
50	0.9334	0.8355	0.3101
65	0.4990	0.8224	0.2124
80	0.2730	0.8090	0.1541

Table 4.10, The adsorbed volumes (V_P) of m-xylene at different

temperatures and maximum relative pressures.

Temperature (°C)	Maximum relative pressure	Density (g/ cm^3)[73]	V_P (cm^3/g)
30	0.9266	0.8553	0.2287
50	0.8774	0.8382	0.2542
65	0.4596	0.8249	0.2323
80	0.2506	0.8114	0.1898

Table 4.11, The adsorbed volumes (V_P) of o-xylene at different temperatures and maximum relative pressures for fresh MCM-41 sample.

Temperature (°C)	Maximum relative pressure	Density (g/cm^3)[73]	V_P (cm^3/g)
30	0.9468	0.8701	0.2753
50	0.9107	0.8526	0.2625
65	0.4562	0.8397	0.2321
80	0.2455	0.8267	0.1707

Since can be reached to high relative pressure at 30°C and 50°C so, we took the V_P values at these temperatures. At the maximum relative pressures (P/Po=0.9334 for p-xylene, P/Po=0.9266 for m-xylene, and P/Po=0.9468 for o-xylene) the volume of liquid sorbates amounts was 0.2365 cm^3/g for p-xylene, 0.2287 cm^3/g for m-xylene, and 0.2753 cm^3/g for o-xylene which is significantly lower than that of pore volume (0.45 cm^3/g) determined by nitrogen adsorption at 77K. The reason of this difference is that the density of the adsorbed phase is unlikely to be exactly the same as that of the liquid adsorptive and slope of isotherms at high relative pressure leads to uncertainty in the location of the upper limit for pore filling. Branton et al. observed similar behavior for physisorption of alcohols and water vapour by MCM-41[31].

4.3 Sorption of ethylbenzene on MCM-41

The sorption capacities of ethylbenzene on MCM-41, which has kinetic diameter (6.0 Å)[4] at different temperatures (30°C, 65°C, 80°C) were presented in Figures 4.16- 4.18 and tables (B.37-B.44).
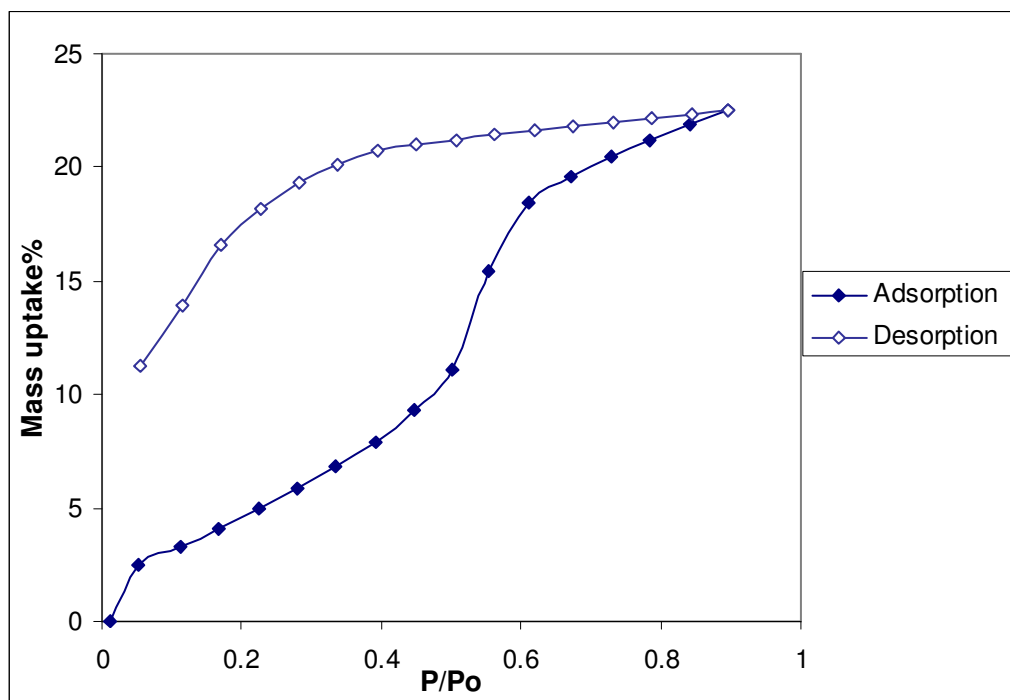
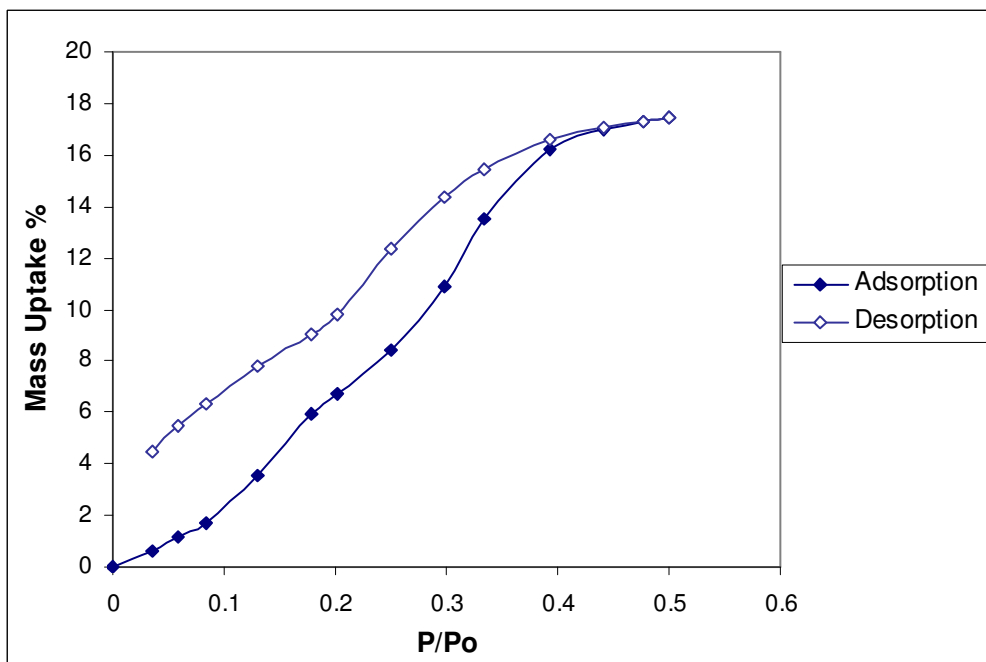Figure 4.16, Adsorption isotherm of ethylbenzene on MCM-41at 30 °C.
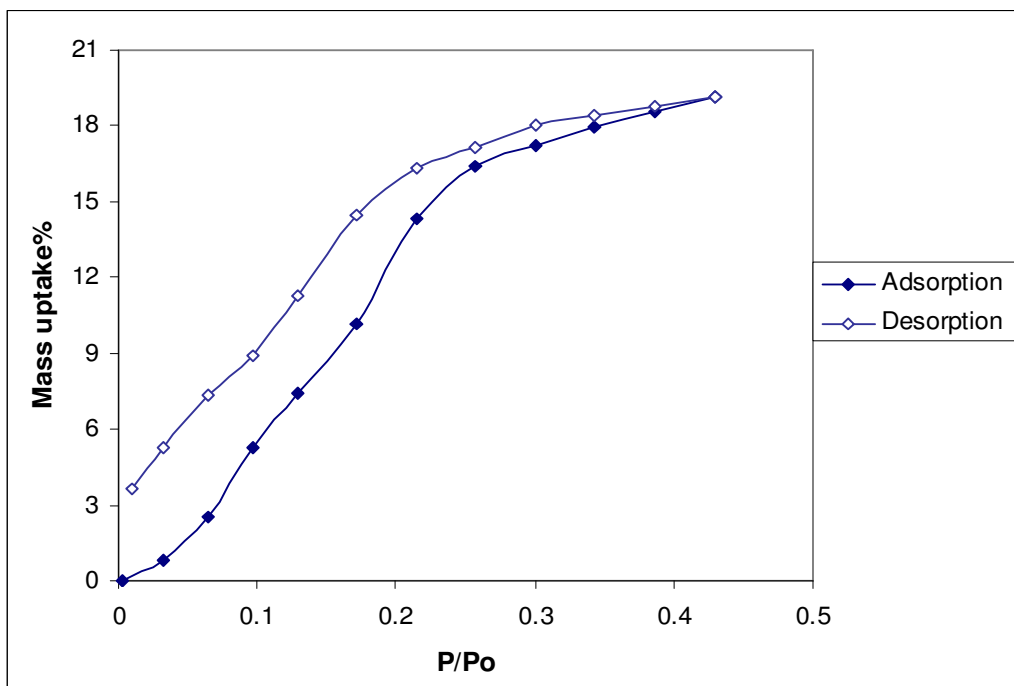
Figure 4.17, Adsorption isotherm of ethylbenzene on MCM-41 at 65 °C.
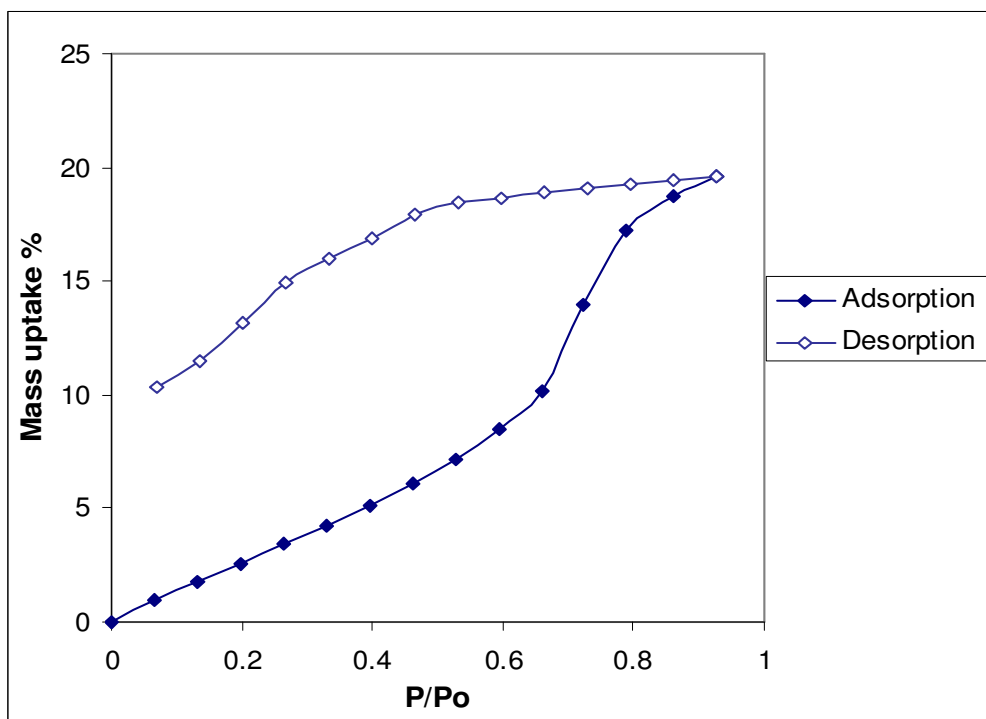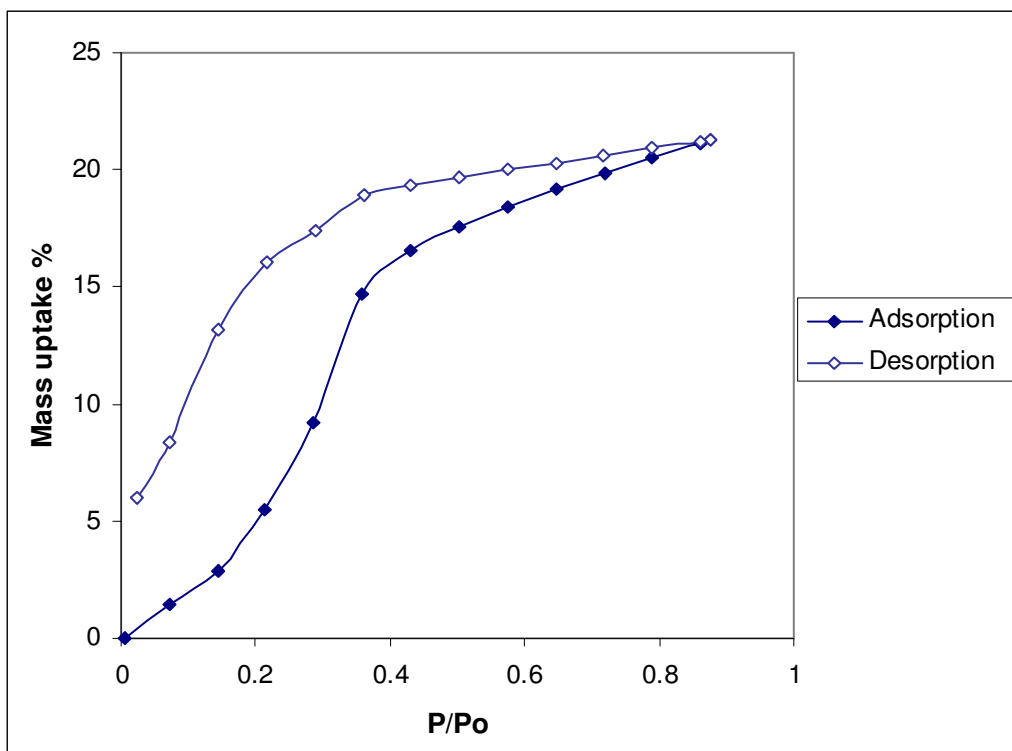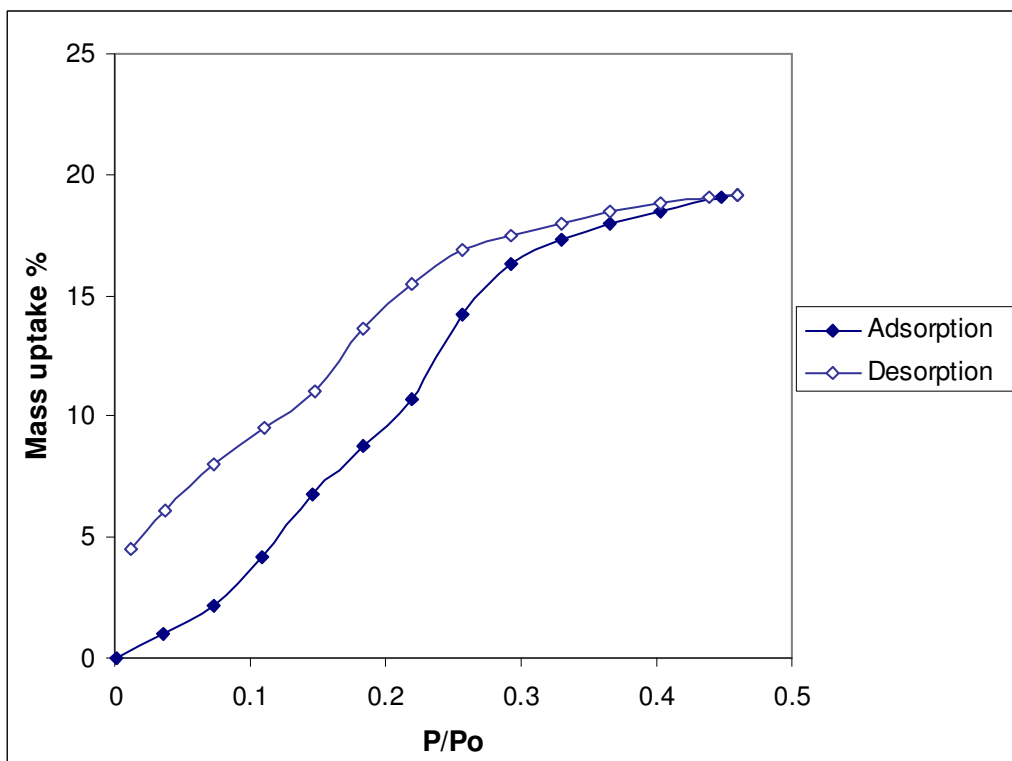

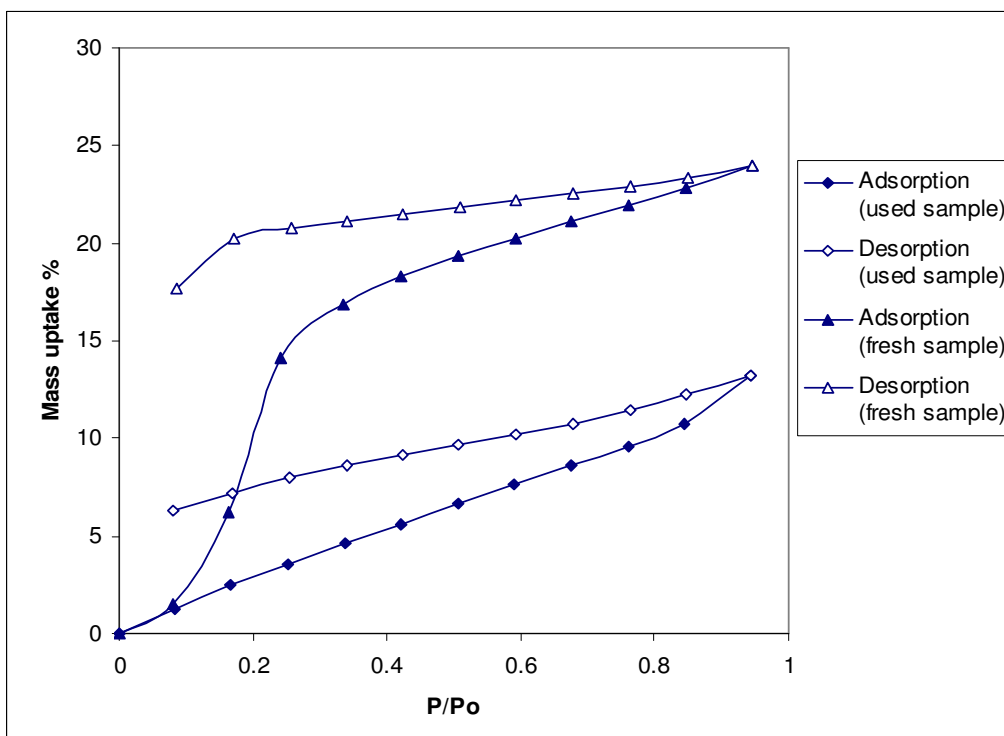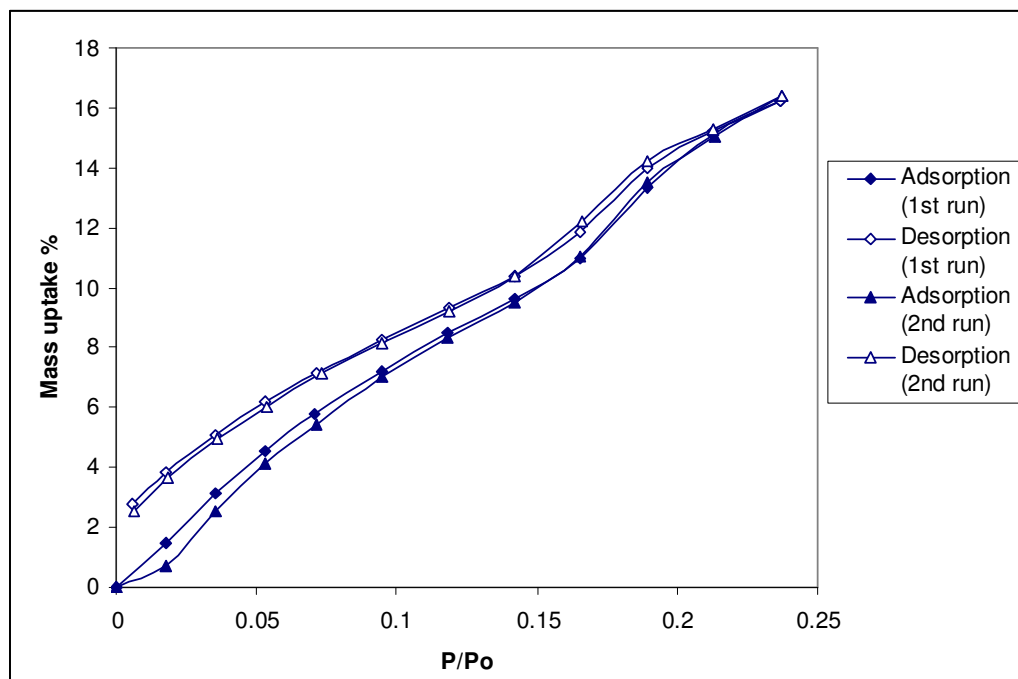Figure 4.18, Comparison of adsorption isotherms for ethylbenzene
at 80°C

As seen from Table (4.12) we could reach to a relatively high relative pressure at 30°C and 50°C, while we could not reach to high relative pressure at 65°C, and 80°C for the same reason for the other sorbates which is to prevent condensation.

Table 4.12 Equilibrium sorption capacities for ethylbenzene.

Temperature (°C)	Maximum pressure(milibars)	Total mass (miligrams)	Maximum relative pressure	Mass uptake %
30	15.9536	24.3135	0.8974	22.4799
65	39.9922	23.9406	0.4296	19.1288
80	39.9364	23.1457	0.2367	16.2522

The amounts of ethylbenzene adsorbed on MCM-41 decreases when the temperature of the adsorption isotherms increases for the same pressure value (Figure A.3 and Table 4.13). The decrease of adsorbed amounts is due to the decrease of density of the sorbate with the increase of adsorption temperature and due to the adsorption equilibrium of the physical adsorption process. Qiao et al. observed similar behavior for hexane adsorption on MCM-41 [68].

Table 4.13 Comparison of sorption capacities for ethylbenzene at same pressure values

Temperature (°C)	pressure(Milibars)	Total mass (miligrams)	Mass uptake %
30	15.9536	24.3135	22.4799
65	15.9681	22.1384	10.1610
80	15.9629	21.3460	7.21290

From the figures (4.16-4.18) for ethylbenzene the isotherm equilibrium curves were type V according to IUPAC isotherm classification due to the mesoporous nature of the MCM-41sample (have an average pore diameter 25Å). The capillary condensation-evaporation within a narrow distribution of mesopores was associated with each adsorption isotherms. Hysteresis associated with capillary condensation-evaporation cycle. The absence of a hysteresis loop can be offered as follows. In MCM-41 sample, pores are believed to be very long compared to their diameters. It is then very likely that the radius is not constant as the pore length, but rather there may be some constrictions caused by imperfections of the pore wall. It is possible that such defects may act as the nuclei for the adsorbate to adsorb at the constrictions and this may divide the through pore into two blind pores. It is understood that adsorption in blind pores is reversible because as adsorption proceeds, a hemispherical meniscus is formed at the bottom of the pore, and subsequent adsorption will occur through this gas-liquid interface. In pores of larger radii, the formation of a meniscus during the adsorption step due to the imperfections of the pore wall is less likely; therefore adsorption in MCM-41 with larger pores is more often accompanied by a hysteresis loop [33]. It was shown that as the temperature for the adsorption isotherms increase the size of hysteresis decrease. hysteresis was shown clearly among all adsorption isotherms curves.

As seen from Figure (A.3) as the temperature of adsorption isotherms increases the values of pressure (or relative pressure for a given adsorption isotherm curve) for the same value of total mass adsorbed of ethylbenzene increases. The large shift of the phase transition from low to high relative pressures originates from the decrease of the surface

tension as temperature increase, that is, it needs higher pressure to achieve the capillary adsorption phase transition at the lower surface tension.

The adsorbed volume (V_P) for ethylbenzene in Table 4.14 have been obtained from the amounts adsorbed at different maximum relative pressures by assuming that the pores are filled with condensed sorbate in the normal liquid state.

Table 4.14, The adsorbed volumes (V_P) of ethylbenzene at different temperatures and maximum relative pressures.

Temperature °C	Relative pressure	Density (g / cm^3)[73]	V_P (cm^3/g)
30	0.8974	0.8586	0.2617
65	0.4296	0.8275	0.2311
80	0.2367	0.8136	0.1997

At maximum relative pressure (P/Po=0.8974) the volume of liquid sorbate amount was 0.2617 cm^3/g which is significantly lower than that obtained from low-temperature nitrogen isotherm (V_P =0.45 cm^3/g). The reason of this difference is that the density of the adsorbed phase is unlikely to be exactly the same as that of the liquid adsorptive and slope of isotherms at high relative pressure leads to uncertainty in the location of the upper limit for pore filling. Branton et al. observed similar behavior for physisorption of alcohols and water vapour by MCM-41[31].

Isosteric heat of adsorption for all sorbates were calculated from the measured adsorption equilibrium data at isotherm temperatures using the Clausius-Clapeyron equation (equation C.3). As seen in Table 4.15 different values of isosteric heat reflect different interaction between these adsorbates with the surface of the pores of MCM-41 sample. Hachimi et al. study the heat of asorption of adsorbed o-xylene on silica by using Temperature Progammed Adsorption Equilibrium methods and he found that o-xylene forms weakly adsorbed species on different silica solids [77-79].

Table 4.15 Isosteric heats of adsorption of C_8 hydrocarbons over various adsorbents

Adsorbate	Adsorbent	Heat of adsorption (kJ/mole)	Reference
o-xylene	MCM-41	- 23.18	This work
m-xylene	MCM-41	- 30.61	This work
p-xylene	MCM-41	- 44.00	This work
ethylbenzene	MCM-41	- 22.40	This work
o-xylene	SiO_2	- 61.00	[77]
p-xylene	SiO_2	- 47.00	[78]
m-xylene	Al_2O_3	- 52.00	[79]

CHAPTER 5

CONCLUSION AND RECOMMENDATIONS

The main purpose of this study was to investigate the sorption equilibrium of C_8 aromatics (o-xylene, p-xylene, m-xylene, and ethylbenzene) on MCM-41 at different temperatures (30°C, 50°C, 65°C, 80°C). MCM-41 was characterized by using XRD and nitrogen physisorption analysis.

Based on the experimental studies the following concluding remarks are obtained:

From nitrogen adsorption isotherms, it was found BET surface area as (492.2 m^2/g), with an average pore diameter (25 Å). The low surface area may be due to the fewer defects in MCM-41 sample, on the other hand, when we compare it with other work in literatures Choma et al. (2003) found BET surface area for MCM-41 sample (465 m^2/g) by using the same synthesized method and the same surfactant [32] (i.e., CTMABr).

MCM-41 sample have the highest sorption capacity for p-xylene, while it was less for the other sorbates at the same temperature. At 65°C, and 80°C we could not reach a high relative pressure to prevent the condensation in the chamber due to limitation that pressure can not exceed vapour pressure at 50°C which is the maximum temperature of chamber.

The amounts of sorbates adsorbed on MCM-41 decreases when the temperature of the adsorption isotherms increases for the same pressure

value. The decrease of adsorped amounts is due to the decrease of density of the sorbates with the increases of temperatures and due to the adsorption equilibrium of the physical adsorption process. The adsorbed amounts was increased for o-xylene by using fresh MCM-41 sample for all the adsorption isotherm experiments at different temperatures. Different values of heat of adsorption reflect different interaction between adsorbates and silica surface. The capillary condensation-evaporation within a narrow distribution of mesopores was associated with each adsorption isotherms and for all sorbates, resulting in hysteresis. It was shown that as the temperatures for the adsorption isotherms increases the size of hysteresis decrease.

Based on the present study, following can be recommended.

This study can be extended by using other sorbates such as CO_2 to examine the sorption properties of MCM-41 as adsorbents.

New MCM-41 sample with high surface area can be used.

REFERENCES

1. Gregg, S. J. and Sing, K. S., "Adsorption, surface area and porosity" Academic press: London, 1967, (p. 2-121).

2. Sing, K. S. W., Everett, D. H., Haul, R. A. W. , Moscou, L., Pierotti, R.A. , Rouquerol, J., Siemieniewska, T., Pure Appl. Chem. 1985, 57, 603-619.

3. Anderson, R.A., "Molecular Sieve Adsorbent Application State of Art" PP 637- 650, Molecular Sieve II, ACS Symposium Series 40, University of Chicago press, Chicago. 1977

4. Öztin, A. " Sorption properties of a high silica zeolite ZSM-35" M.Sc. Thesis in Ch.E., M.E.T.U., Ankara, 1997

5. Karge, H.G., Weitkamp, J., "Molecular sieves synthesis" 1st edition, Springer-Verlag, Newyork, 97-118 (1998)

6. Myers, D., Surfactant Science and Technology , 2nd ed., 1992, 28, 7, 936

7. Lawrence, M. J., Surfactant Systems: Their use in drug delivery, Chem. Soc. Rev. 1994, 23, 417-424.

8. Meynen, V., Cool, P., Vansant, E. F., Verified syntheses of mesoporous materials, Microporous Mesoporous Mater., 125 (2009) 170-223.

9. Øye, G., Sjoblom, J., Stocker, M., "Synthesis, characterization and Potential applications of new materials in the mesoporous range", Adv. Colloid Interface Sci., 2001, 89-90, 439-466

10. Vartuli, J. C., Schmitt, K. D., Kresge, C. T., Roth, W. J., Leonowicz, M. E., McCullen, S. B., Hellring, S. D., Beck, J. S.,

Schlenker, J. L., Olson, D. H., Sheppard, E. W., Effects of surfactant/Silica Molar Ratios on the Formation of Mesoporous Molecular Sieves: Inorganic Mimicry of surfactant liquid- crystal phases and mechanistic implications. Chem. Mater. 1994, 6, 2317-2326.

11. Monnier, A., Schuth, F., Huo, Q., Kumar, D., Margolese, D., Maxwell, R. S., Stucky, G. D., Krishnamurthy, M., Petroff, P., Firouzi, A., Janicke, M., Chmelka, B. F., Cooperative formation of inorganic- organic interfaces in the synthesis of silicate Mesostructures, Science , 1993, 261, 1299-1303.

12. Anderson, M. W., Simplified description of MCM-48 Zeolites, 1997, 19, 220-227

13. Schumacher, K., Grun, M., Unger, K. K.," Novel synthesis of spherical MCM-48", Microporous Mesoporous Mater., 1999, 27, 201-206

14. Glanville, Y. J., Pearce, J. V., Sokol, P. E., Newalker, B., Komarneni, S., "Study of H_2 confined in highly ordered pores of MCM-48", Chemical Physics, 292: 289-293 (2003)

15. Huo, Q., Margolese, D. I., Stucky, G. D., Surfactant control of phases in the synthesis of mesoporous silica-based materials, Chem. Mater. 1996, 8, 1147

16. Güçbilmez, Y., Dogu, T., Balci, S., "Vanadium incorporated high surface area MCM-41 catalysts" Catalysis Today, 100: 473-477(2005).

17. Behrens, P., Glaue, A., Haggenmtiller, Schechner, G., Structure-directed materials synthesis : synthesis field diagrams for the

preparation of mesostructured silicas, Solid State Ionics 1997, 101-103, 255-260

18. Brunauer, S., Deming, L., Deming, W., Teller, E., J. Am. Chem. Soc. 62 (1940) 1723.

19. Karslı H., "Adsorption properties of ferrierite and silicalite ", M. S. Thesis in Ch. E., M.E.T.U. , Ankara, 1990.

20. Isotherm classifications. Prof. Dr. Marc Donohue, Department of Chemical Engineering, Johns Hopkins University.

21. Parasuraman Selvam, Suresh K. Bhatia, and Chandrashekar G. Sonwane, Recent advances in processing and characterization of periodic mesoporous MCM-41 silicate molecular sieves, Ind. Eng. Chem. Res., 2001, 40(15), 3237-3261.

22. Corma, A., Microporous to Mesoporous Molecular Sieve Materials and Their Use in Catalysis, Chem. Rev. 1997, 97, 2373.

23. Corma, A., Kumar, D., Possibilities of Mesoporous Materials in Catalysis, Stud. Surf. Sci. Catal. 1998, 117, 201.

24. Sayari, A., Catalysis by Crystalline Mesoporous Molecular Sieves. Chem. Mater. 1996, 8, 1840.

25. Sheldon, R. A., Wallau, M., Arends, M., Schuchardt, I. W. C. E., Heterogeneous Catalysts for Liquid-Phase Oxidations: Philosopher´s stones or Trojan horses? Acc. Chem. Res. 1998, 31, 485.

26. Suzuki, N., Asami, H., Nakamura, T., Huhn, T., Fukuoka, A., Ichikawa, M., Saburi, M., Wakatsuki, Y. Immobilization of a C2-symmetric Ansa-zirconocene complex on silica surfaces Using a Si-Cl Anchor: catalysts for isospecific propene polymerization. Chem. Lett. 1999, 4, 341.

27. Sheldon, R. A., Homogeneous catalysts to solid catalysts. Curr. Opin. Solid state mater. Sci. 1996, 1, 101.

28. Kresge, C. T., Leonowicz, M. E., Roth, W. J., Vartuli, J. C., Beck, J. S., Ordered mesoporous molecular sieves synthesized by a liquid- crystal template mechanism. Nature 1992, 359, 710.

29. Beck, J. S., Vartuli, J. C., Roth, W. J., Leonowicz, M. E., Kresge, C. T., Schmitt , K. D., Chu, C. T. W., Olsen, D. H., Sheppard, E. W., McCullen, S. B., Higgins, J. B., Schlenker, J. L., A new family of mesoporous molecular sieves prepared with liquid crystal templates., J. Am. Chem. Soc. 1992, 114, 10835.

30. Branton, P. J., Hall, P. J., and Sing, S. W. K., Reichert, H., Schüth, F., and Unger, K. K., Physisorption of argon, nitrogen, and oxygen by MCM-41, a model mesoporous adsorbent., J. Chem. Soc. Faraday Trans., 1994, 90(19), 2965-2967.

31. Branton, P. J., Hall, P. J., and Sing, S. W. K., "physisorption of alcohols and water vapour by MCM-41, a model mesoporous adsorbent". Adsorption, 1, 77-82 (1995).

32. Choma, J., Kloske, M., Jaroniec, M., Klinik, J., "Benzene adsorption isotherms on MCM-41 and their use for pore size analysis", Adsorption 10: 195-203, 2004.

33. Nguyen, C., Sonwane, C. G., Bhatia, S. K., Do, D. D. "Adsorption of Benzene and Ethanol on MCM-41 Materials", Langmuir 1998, 14, 4950-4952.

34. Rathousky, J., Zukul, A., Franke, O., Schulz-Ekloff, G., Adsorption on MCM-41 Mesoporous Molecular Sieves, Part 2. Cyclopentane Isotherm and Their Temperature Dependence, J. Chem. Soc. Faraday Trans., 1995, 91, 937.

35. Gruün, M., Kurganov, A. A., Schacht, S., Schüüth, F., Unger, K. K., Comparison of an Ordered Mesoporous Aluminosilicate Silica, Alumina, Titania and Zirconia in Normal-Phase High-Performance Liquid Chromatography, J. Chromatogr. A 1996, 740, 1.

36. Gruün, M., Lauer, I., Unger, K. K., The synthesis of micrometer- and submicrometer-size spheres of ordered mesoporous oxide MCM-41. Adv. Mater. 1997, 9, 254.

37. Raimondo, M., Sinibaldi, P. M., De Stefanis, A., Tomlinson, A. A. G., Mesoporous M41S Materials in Capillary Gas Chromatogaraphy., Chem. Commun. 1997, 1343.

38. Xu, Y. M., Wang, R. S., Wu, F., Surface Characters and Adsorption Behavior of Pb(II) onto a Mesoporous Titanosilicate Molecular Sieve,. J. Colloid Interface Sci.1999, 209, 380.

39. Wilson, E., Coated Mesoporous Silica: Supersoaker for Heavy Metals, Chem. Eng. News 1997, 5, 46.

40. Mercier, L.; Pinnavaia, T. J., Access in Mesoporous Materials: Advantages of a Uniform Pore Structure in the Design of a Heavy Metal Ion Adsorbent for Environmental Remediation, Adv. Mater. 1997, 9, 500.

41. Feng, X., Fryxell, F. E., Wang, I. Q., Kim, A., Liu, J., Kemnere, K. M., Functionalized monolayers on ordered mesoporous supports. Science 1997, 276, 923.

42. Brown, J., Richer, R., Mercier, L., One-Step Synthesis of High-Capacity Mesoporous Hg^{2+} Adsorbents by Nonionic Surfactant Assembly, Microporous Mesoporous Mater. 2000, 37, 41.

43. Moller, K., Bein, T., Inclusion Chemistry in Periodic Mesoporous Hosts, Chem. Mater. 1998, 10, 2950.

44. Ozin, G. A., Nanochemistry: Synthesis in Diminishing Dimensions, Adv. Mater. 1992, 10, 612.

45. Selvam, P., Badamali, S. K., Murugesan, M., Kuwano, H., Superparamagnetic Particles in Mesoporous FeMCM-41 Molecular Sieves. Recent Trends in catalysis, Murugesan, V., Arabindo, B., Palanichamy, M., Eds., Narosa: New Delhi, 1999, p-545.

46. Llewellyn, P. L., Ciesla, U., Decher, H., Stadler, R., Schüth, F., Unger, K. K., MCM-41 and Related Materials as Media for Controlled Polymerization Processes, Stud. Surf. Sci. catal. 1994, 84, 2013.

47. Leon, R., Margolese, D., Stucky, G., Petroff, P. M., Nanocrystalline Ge filaments in the pores of a mesosilicate, Phys. Chem. B 1999, 103, 4228.

48. Beck, J. S., Kresge, C. T., McCullen, S. B., Roth, W.J., Vartuli, J.C., U. S. Patent, 5, 304, 363, 1994.

49. Kresge, C. T., Leonowicz, M. E., Roth, W. J., Vartuli, J. C., and Beck, J. S., Nature, 1992, 359,710.

50. Beck, J. S., Vartuli, J. C., Roth, W. J., Leonowicz, M. E., Kresge, C. T., Schmitt, K. D., Chu, T. T.-W., Olson, D. H., Sheppard, E. W., McCullen, S. B., Higgins, J. B., and Schlenker, J. L., J. Am. Chem. Soc., 1992, 114, 10834.

51. Beck, J. S., U. S. Patent, 5, 057, 296, 1991.

52. Beck, J. S., Socha, R. F., Shihabi, D. S., Vartuli, J. C., U. S. Patent, 5, 143, 707, 1992.

53. Kresge, C. T., Leonowicz, M. E., Roth, W. J., Vartuli, J. C., U. S. Patent, 5, 098, 684, 1991.

54. Collart, O., "Nanodesign of an Aluminasilicate Framework in Mesoporous MCM-48 Architecture", PhD Thesis, University of Antwerpen, 2003.

55. Raman, N. K., Anderson, M. T., Brinker, C. J. Chem. Mater. 1996, 8, 1682.

56. Sayari, A., Liu, P. Microporous Mater. 1997, 12, 149.

57. Ciesla, U.,Schuth,F. Microporous Mesoporous Mater. 1999,27,131

58. Selvam, P., Bhatia, S. K., Sonwane, C. G. Ind. Eng. Chem. Res. 2001, 40, 3237.

59. Choma, J., Jaroniec, M., Michalski, M., and Kloske, M., "characterization of ordered Nanoporous materials on the basis of argon Adsorption", Ochrona Srodowiska, 24, 3-9 (2002b) (in Polish).

60. Russo, P. A., M. Manuela L. Ribeiro Carrott, Peter J. M. Carrott "Adsorption of toluene, methylcyclohexane, and neopentane on silica MCM-41", Adsorption, 14: 367-375 (2008).

61. Priti A. Mangrulkar, Sanjay P. kamble, J. Meshram. Sadhana S. Rayalu, "Adsorption of phenol and o-chlorophenol by mesoporous MCM-41", Journal of hazardous materials 160 (2008) 414-421.

62. Qin, Q., Ma, J., Liu, K., "Adsorption of nitrobenzene from aqueous solution by MCM-41", Science Direct, journal of colloid and interface science 315 (2007) 80-86.

63. Monash, P., Majhi, A., Pugazhenthi, G., "Adsorption studies of methylene blue onto MCM-41", the 12th international conference

of international association for computer methods and advances in geomechanics (IACMAG) 1-6 October, 2008, Goa, India.

64. IGA systems user manual.

65. Yaw´s Handbook of Antoine coefficients for vapour pressure, Carl L. Yaws,
http://aichemembers.knovel.com/knovel2/Toc.jsp?BookID=1183
Last access, 30, May, 2010.

66. JCPDS- International center for Diffraction Data, 2002, 49-1712.

67. She-Tin Wong, Hong-Ping Lin, Chung-Yuan Mou, "Tubular MCM-41- supported transition metal oxide catalysts for ethylbenzene dehydrogenation reaction", Applied Catalysis A: General 198 (2000) 103-114.

68. Qiao, S. Z., Bhatia, S. K., and Nicholson, D., "Study of hexane adsorption in nanoporous MCM-41 silica", Langmuir, 2004, 20 (2), 389-395.

69. Roth, W. J., Synthesis of the Cubic Mesoporous Molecular Sieve MCM-48, 2000, US Patent No. 6, 096, 288.

70. Slomaz, A., "Synthesis and characterization of MCM-41 catalysts activated with vanadium, molybdenum and niobium" M. Sc. Thesis, Gazi University, Institute of science and technology, June, 2007.

71. Everett, D. H., in characterization of porous solids, Proc. Int. Symp. 1978, ed. Gregg, S. J., Sing, K. S. W. and Stoeckli, H. F., Society of chemical industry, London, 1979, p. 107.

72. Burgess, C. G. V., Everett, D. H., and Nuttall, S., Pure Appl. Chem., 1989, 61, 1845.

73. DDBST,

http://www.ddbst.com/en/online/Online_Calc_den_Form.php
Last access, 30, May, 2010.

74. IUPAC Recommendations, Pure Appl. Chem., 66 (1994) 1739.

75. Şener C. "Synthesis and characterization of pd-MCM-Type mesoporous nanocomposite materials" M. Sc. Thesis in Ch.E., M.E.T.U., Ankara, 2006.

76. IUPAC Recommendations, Pure Appl. Chem., 57 (1985) 603.

77. Abdouelilah Hachimi, Tarik Chafik and Daniel Bianchi, Adsorption models and heat of adsorption of adsorbed ortho di-methyl benzene species on silica by using Temperature Programmed Adsorption Equilibrium methods. Applied Catalysis A: General, 335, 2, 2008, p 220-229.

78. M.A. Hernandez, J.A. Velasco, M. Asomoza, S. Solis, F. Rojas and V.H. Lara, Ind. Eng. Chem. Res. 43(2004), p. 1779.

79. L.H. Kelmm and S.K. Airee, J. Chromatogr. 13 (1964), p. 40.

APPENDIX A

COMPARISON OF ADSORPTION ISOTHERMS FOR ALL
SORBATES AT ALL TEMPERATURES
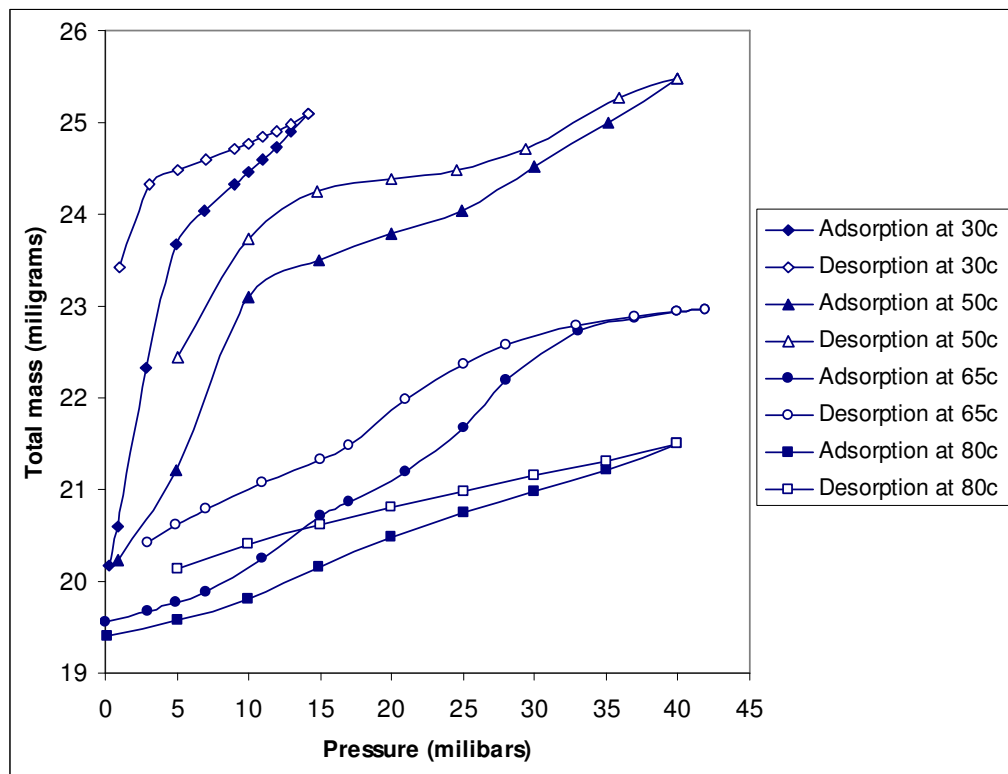
Figure A.1, Comparison of adsorption isotherms for p-xylene at all temperatures.
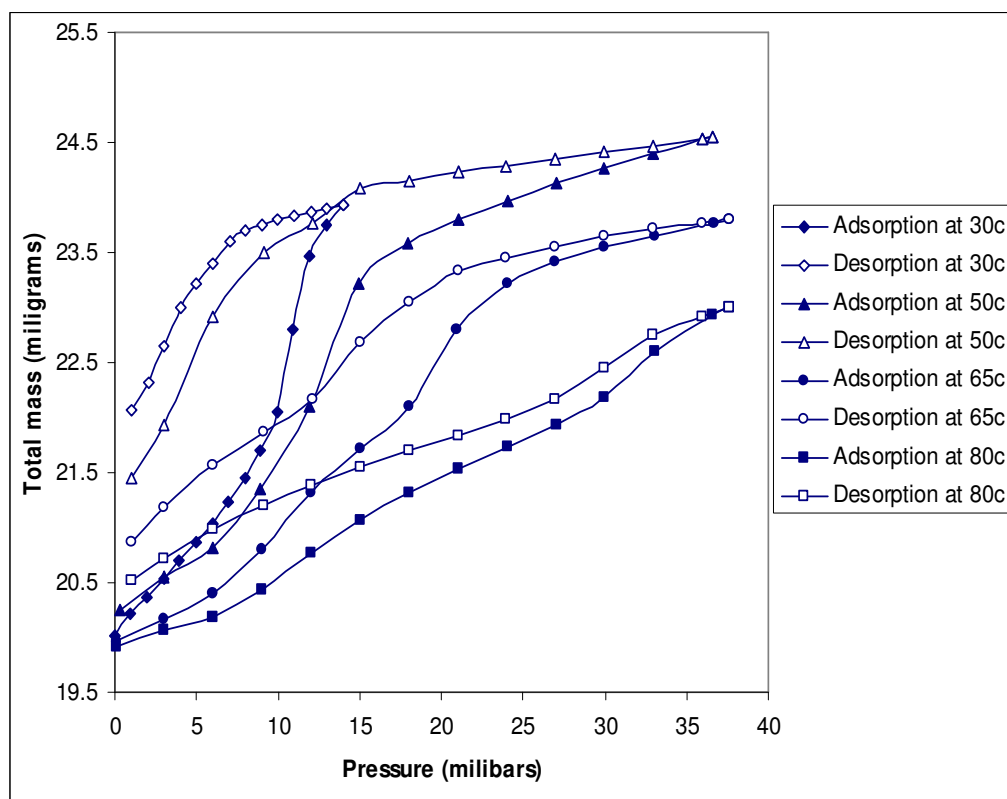
Figure A.2, Comparison of adsorption isotherms for m-xylene at all temperatures.
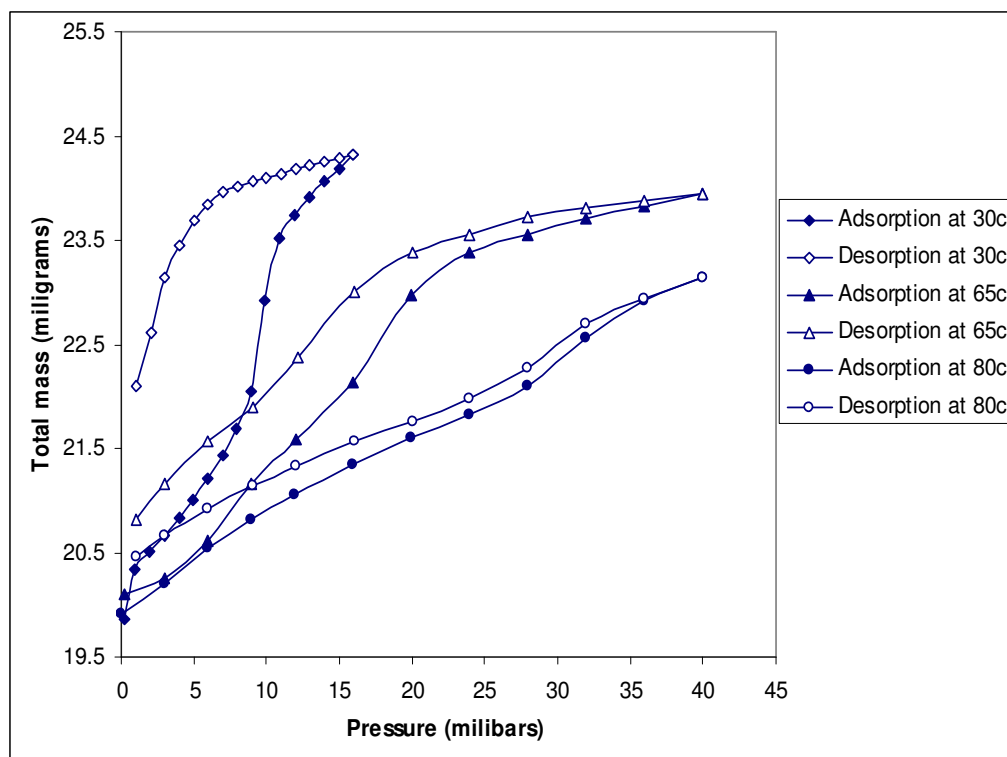
Figure A.3, Comparison of adsorption isotherms for ethylbenzene at all temperatures.
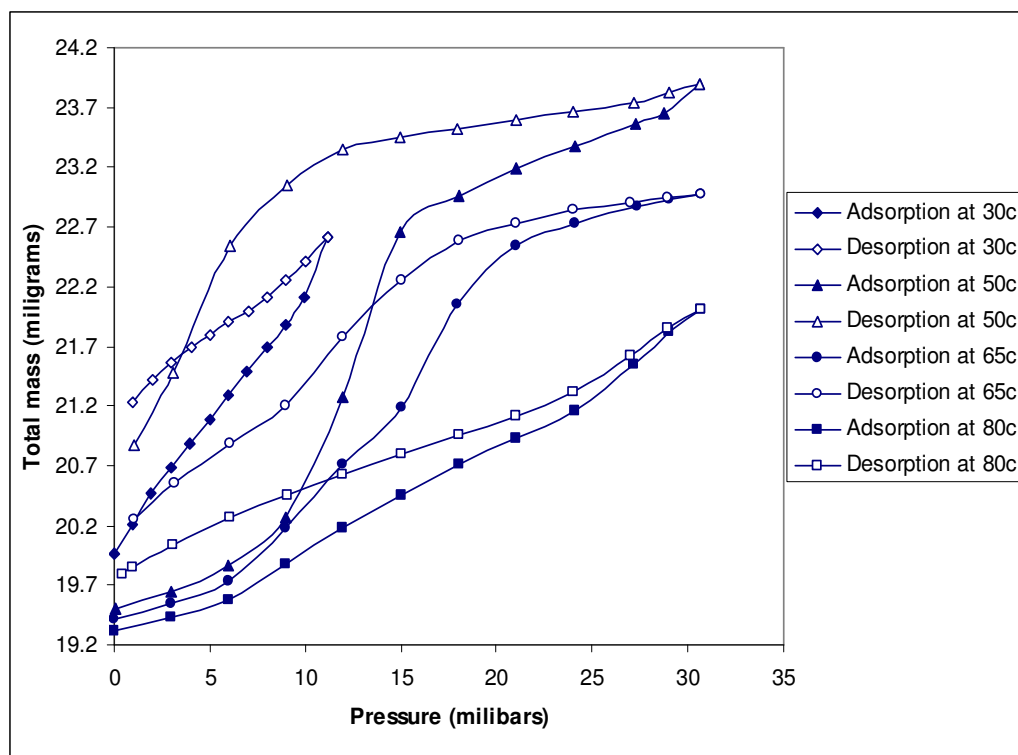
Figure A.4, Comparison of adsorption isotherms for o-xylene at all temperatures (used sample).
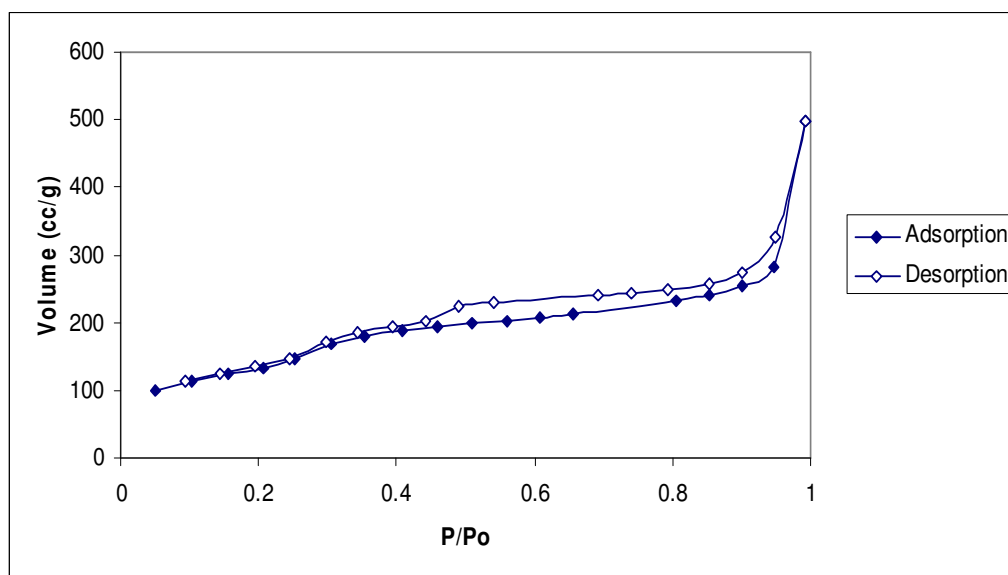
Figure A.5 Nitrogen adsorption isotherm of MCM-41 sample after the 1st calcination
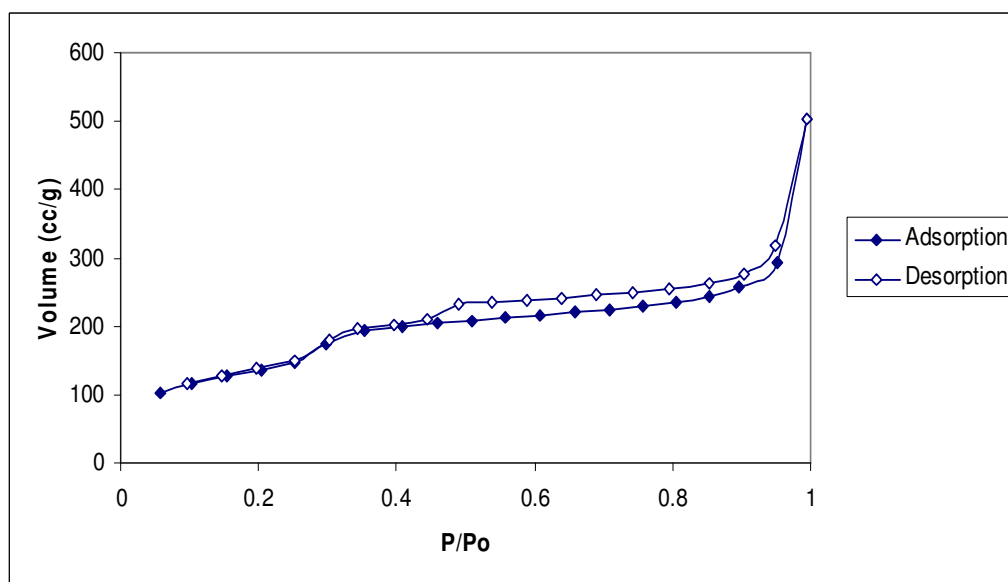
Figure A.6 Nitrogen adsorption isotherm of MCM-41 sample after the 2nd calcination

APPENDIX B

ADSORPTION ISOTHERMS DATA FOR ALL SORBATES

Table B.1, Data for p-xylene adsorption isotherm at 30°C (Adsorption).

Pressures (Milibars)	Total mass (Miligrams)	Relative Pressure(P/Po)	Mass uptake % $((Wt-Wto)/Wto)$
0.0000	20.175	0.0000	0.0000
0.9188	20.592	0.0591	2.0650
2.8259	22.322	0.1810	10.6380
4.9122	23.6791	0.3163	17.3632
6.9323	24.0449	0.4463	19.1763
8.9420	24.3273	0.5757	20.5760
9.9553	24.4672	0.6410	21.2694
10.9490	24.6054	0.7050	21.9544
11.9541	24.7401	0.7697	22.6220
12.9577	24.8961	0.8343	23.3952
14.1490	25.1042	0.9110	24.4266

Table B.2, Data for p-xylene adsorption isotherm at 30 °C (Desorption).

Pressures (Milibars)	Total mass (Miligrams)	Relative Pressure(P/Po)	Mass uptake % $((Wt-Wto)/Wto)$
14.1490	25.1042	0.9110	24.4266
12.9895	24.9899	0.8364	23.8601
11.9907	24.9084	0.7720	23.4562
10.9926	24.8374	0.7078	23.1043
10.0123	24.7730	0.6447	22.7851
9.0082	24.7108	0.5800	22.4768
7.0094	24.5946	0.4513	21.9008
5.0242	24.4740	0.3235	21.3031
3.0305	24.3241	0.1951	20.5601
1.0163	23.4160	0.0654	16.0592

Table B.3, Data for p-xylene adsorption isotherm at 50°C (Adsorption).

Pressures (Milibars)	Total mass (Miligrams)	Relative Pressure(P/Po)	Mass uptake % $((Wt-Wto)/Wto)$
0.0000	20.2291	0.0000	0.00000
4.9764	21.2187	0.1162	4.89196
9.9713	23.0913	0.2329	14.14892
14.9618	23.5036	0.3494	16.18708
19.9718	23.7939	0.4665	17.62214
24.9211	24.0460	0.5821	18.86836
29.9640	24.5209	0.6999	21.21597
35.1337	24.9990	0.8206	23.57940
39.9607	25.4715	0.9334	25.91514

Table B.4, Data for p-xylene adsorption isotherm at 50°C (Desorption).

Pressures (Milibars)	Total mass (Miligrams)	Relative Pressure(P/Po)	Mass uptake % $((Wt-Wto)/Wto)$
39.9607	25.4715	0.933421	25.91514
35.8205	25.2618	0.836713	24.87852
29.3473	24.7172	0.685508	22.18636
24.5925	24.4814	0.574443	21.02071
20.0252	24.3883	0.467758	20.56048
14.8321	24.2428	0.346455	19.84122
10.0236	23.7373	0.234136	17.34234
5.0260	22.4519	0.117400	10.98813

Table B.5, Data for p-xylene adsorption isotherm at 65°C (Adsorption).

Pressures (Milibars)	Total mass (Miligrams)	Relative Pressure(P/Po)	Mass uptake % $((Wt-Wto)/Wto)$
0.0000	19.5513	0.0000	0.000000
2.9918	19.6704	0.0356	0.609167
4.9788	19.7714	0.0593	1.125756
6.9964	19.8890	0.0834	1.727251
10.9863	20.2455	0.1310	3.550659
14.9934	20.7113	0.1787	5.933109
16.9920	20.8615	0.2026	6.701345
20.9846	21.1978	0.2502	8.421435
24.9792	21.6788	0.2978	10.88163
27.9808	22.1880	0.3336	13.48606
32.9880	22.7278	0.3933	16.24700
36.9716	22.8699	0.4408	16.97381
39.9815	22.9371	0.4767	17.31752
41.9260	22.9677	0.4999	17.47403

Table B.6, Data for p-xylene adsorption isotherm at 65°C (Desorption).

Pressures (Milibars)	Total mass (Miligrams)	Relative Pressure(P/Po)	Mass uptake % $((Wt-Wto)/Wto)$
41.9260	22.9677	0.499940	17.47403
39.9710	22.9393	0.476628	17.32877
36.9590	22.8846	0.440712	17.04899
32.9791	22.7926	0.393254	16.57844
27.9875	22.5737	0.333733	15.45882
24.9907	22.3571	0.297998	14.35096
20.9931	21.9717	0.250329	12.37974
16.9952	21.4723	0.202657	9.825434
14.9955	21.3233	0.178812	9.063336
10.9871	21.0748	0.131014	7.792321
6.99860	20.7874	0.083454	6.322342
4.98250	20.6183	0.059413	5.457438
2.99360	20.4282	0.035697	4.485124

Table B.7, Data for p-xylene adsorption isotherm at 80 °C
(1st run, Adsorption).

Pressures (Milibars)	Total mass (Miligrams)	Relative Pressure(P/Po)	Mass uptake % $((Wt - Wto)/Wto)$
0.0000	19.4890	0.0000	0.000000
2.9930	19.5925	0.0194	0.531069
4.9899	19.6614	0.0324	0.884602
6.9943	19.7370	0.0454	1.272513
9.9857	19.8755	0.0649	1.983170
12.9836	20.0945	0.0844	3.106881
14.9913	20.2282	0.0974	3.792909
16.9921	20.3547	0.1105	4.441993
20.9920	20.6533	0.1365	5.974139
24.9843	20.9134	0.1624	7.308738
27.9799	21.0773	0.1819	8.149725
29.9553	21.1639	0.1948	8.594079
31.9452	21.2275	0.2077	8.920417
33.9506	21.2916	0.2207	9.249320
36.9872	21.4410	0.2405	10.01591
39.9950	21.7401	0.2600	11.55062
41.9807	21.9203	0.2730	12.47524

Table B.8, Data for p-xylene adsorption isotherm at 80 °C
(1st run, Desorption).

Pressures (Milibars)	Total mass (Miligrams)	Relative Pressure(P/Po)	Mass uptake % $((Wt - Wto)/Wto)$
41.9807	21.9203	0.273013	12.47524
39.9707	21.7671	0.259942	11.68916
36.9738	21.5586	0.240452	10.61932
33.9764	21.4063	0.220959	9.837857
31.9787	21.3249	0.207967	9.420186
29.9793	21.2544	0.194964	9.058443
27.9859	21.1886	0.182001	8.720817
24.9947	21.0844	0.162548	8.186156
20.9962	20.9406	0.136545	7.448304
16.9932	20.7830	0.110512	6.639643
14.9789	20.6996	0.097412	6.211709
12.9959	20.6134	0.084516	5.769408
10.0000	20.4758	0.065033	5.063369
6.99530	20.3141	0.045493	4.233670
4.98740	20.1927	0.032435	3.610755
1.99760	19.9821	0.012991	2.530145

Table B.9, Data for p-xylene adsorption isotherm at 80°C
(2nd run, Adsorption).

Pressures (Milibars)	Total mass (Miligrams)	Relative Pressure(P/Po)	Mass uptake % $((Wt - Wto)/Wto)$
0.0000	19.4104	0.0000	0.000000
4.99340	19.5719	0.0324	0.832028
9.99000	19.8167	0.0649	2.093208
14.9782	20.1508	0.0974	3.814450
19.9823	20.4712	0.1299	5.465111
24.9695	20.7425	0.1623	6.862816
29.9764	20.9825	0.1949	8.099266
34.9861	21.2168	0.2275	9.306351
39.9893	21.5009	0.2600	10.77000

Table B.10, Data for p-xylene adsorption isotherm at 80 °C
(2nd run, Desorption).

Pressures (Milibars)	Total mass (Miligrams)	Relative Pressure(P/Po)	Mass uptake % $((Wt - Wto)/Wto)$
39.9893	21.5009	0.260063	10.77000
34.9795	21.3026	0.227482	9.748382
29.9896	21.1444	0.195031	8.933355
24.9956	20.9848	0.162554	8.111116
20.0165	20.8132	0.130173	7.227054
15.0123	20.6196	0.097630	6.229650
10.0155	20.4006	0.065134	5.101389
5.02160	20.1328	0.032657	3.721716

Table B.11, Data for m-xylene adsorption isotherm at 30 °C
(Adsorption).

Pressures (Milibars)	Total mass (Miligrams)	Relative Pressure(P/Po)	Mass uptake % $((Wt - Wto)/Wto)$
0.0000	20.0136	0.0000	0.00000
0.9709	20.2107	0.0645	0.98483
1.9741	20.3717	0.1311	1.78928
2.9764	20.5344	0.1977	2.60223
3.9793	20.6988	0.2644	3.42367
4.9752	20.8615	0.3306	4.23661
5.9693	21.0331	0.3966	5.09403
6.9641	21.2256	0.4627	6.05588
7.9529	21.4439	0.5284	7.14664
8.9442	21.7077	0.5943	8.46474
9.9322	22.0462	0.6599	10.1560
10.8813	22.7994	0.7230	13.9195
11.8847	23.4602	0.7897	17.2212
12.9404	23.7557	0.8598	18.6977
13.9449	23.9303	0.9266	19.5701

Table B.12, Data for m-xylene adsorption isotherm at 30 °C
(Desorption).

Pressures (Milibars)	Total mass (Miligrams)	Relative Pressure(P/Po)	Mass uptake % $((Wt - Wto)/Wto)$
13.9449	23.9303	0.926633	19.57019
12.9867	23.9048	0.862961	19.44278
11.9880	23.8695	0.796598	19.26640
10.9944	23.8325	0.730573	19.08152
9.9931	23.7965	0.664037	18.90165
8.9923	23.7519	0.597535	18.67880
7.9907	23.7011	0.530979	18.42497
7.0037	23.6066	0.465393	17.95279
6.0205	23.3955	0.400060	16.89801
5.0141	23.2148	0.333185	15.99512
4.0175	23.0056	0.266961	14.94983
3.0262	22.6506	0.201090	13.17604
2.0345	22.3134	0.135192	11.49119
1.0247	22.0734	0.068091	10.29200

Table B.13, Data for m-xylene adsorption isotherm at 50 °C (Adsorption).

Pressures (Milibars)	Total mass (Miligrams)	Relative Pressure(P/Po)	Mass uptake % $((Wt - Wto)/Wto)$
0.0000	20.2431	0.0000	0.000000
2.9932	20.5423	0.0717	1.478034
5.9853	20.8234	0.1434	2.866656
8.9433	21.3492	0.2142	5.464084
11.9267	22.1058	0.2857	9.201654
14.9014	23.2186	0.3570	14.69884
17.9756	23.5905	0.4306	16.53600
20.9863	23.7978	0.5028	17.56006
23.9919	23.9715	0.5748	18.41813
27.0001	24.1259	0.6468	19.18086
29.9913	24.2664	0.7185	19.87492
32.9896	24.4026	0.7903	20.54774
35.9114	24.5253	0.8604	21.15387
36.6234	24.5566	0.8774	21.30850

Table B.14, Data for m-xylene adsorption isotherm at 50 °C (Desorption).

Pressures (Milibars)	Total mass (Miligrams)	Relative Pressure(P/Po)	Mass uptake % $((Wt - Wto)/Wto)$
36.6234	24.5566	0.877459	21.3085
35.9856	24.5401	0.862178	21.2269
32.9640	24.4747	0.789784	20.9039
29.9746	24.4133	0.718161	20.6006
26.9844	24.3533	0.646519	20.3042
23.9814	24.2913	0.574570	19.9979
20.9950	24.2272	0.503019	19.6812
18.0001	24.1562	0.431264	19.3305
15.0290	24.0774	0.360080	18.9412
12.0869	23.7625	0.289590	17.3856
9.09960	23.4940	0.218017	16.0593
6.04760	22.9151	0.144894	13.1995
3.04220	21.9415	0.072888	8.39001
0.99500	21.4566	0.023839	5.99463

Table B.15, Data for m-xylene adsorption isotherm at 65 °C
(Adsorption).

Pressures (Milibars)	Total mass (Miligrams)	Relative Pressure(P/Po)	Mass uptake % $((Wt - Wto)/Wto)$
0.0000	19.9647	0.0000	0.0000
2.9800	20.1652	0.0364	1.0042
5.9802	20.4031	0.0730	2.1958
8.9715	20.8037	0.1096	4.2024
11.9712	21.3143	0.1462	6.7599
14.9938	21.7228	0.1832	8.8060
17.9934	22.1069	0.2198	10.7299
20.9653	22.8053	0.2561	14.2281
23.9908	23.2133	0.2931	16.2717
26.9912	23.4226	0.3298	17.3200
29.9840	23.5470	0.3664	17.9431
33.0319	23.6522	0.4036	18.4701
36.6591	23.7665	0.4479	19.0426
37.6167	23.7920	0.4596	19.1703

Table B.16, Data for m-xylene adsorption isotherm at 65 °C
(Desorption).

Pressures (Milibars)	Total mass (Miligrams)	Relative Pressure(P/Po)	Mass uptake % $((Wt - Wto)/Wto)$
37.6167	23.7920	0.459682	19.17034
35.9485	23.7645	0.439296	19.03259
32.9641	23.7143	0.402827	18.78115
29.9699	23.6559	0.366237	18.48863
26.9874	23.5575	0.329790	17.99576
23.9824	23.4566	0.293069	17.49037
20.9933	23.3414	0.256541	16.91335
18.0068	23.0539	0.220046	15.47331
15.0412	22.6838	0.183806	13.61954
12.1088	22.1666	0.147971	11.02897
9.0912	21.8681	0.111096	9.533827
6.0274	21.5648	0.073656	8.014646
3.0205	21.1869	0.036911	6.121805
1.0105	20.8598	0.012348	4.483413

Table B.17, Data for m-xylene adsorption isotherm at 80 °C
(1st run, Adsorption).

Pressures (Milibars)	Total mass (Miligrams)	Relative Pressure(P/Po)	Mass uptake % (($Wt - Wto)/Wto$)
0.0000	19.9239	0.0000	0.0000
2.9882	20.0599	0.0198	0.6825
5.9889	20.1913	0.0398	1.3421
8.9862	20.4260	0.0598	2.5200
11.9919	20.7668	0.0798	4.2305
14.9961	21.0625	0.0998	5.7147
17.9926	21.3162	0.1197	6.9880
20.9899	21.5407	0.1397	8.1148
23.9927	21.7385	0.1597	9.1076
26.9971	21.9370	0.1797	10.1039
29.9838	22.1914	0.1996	11.3808
33.0919	22.6007	0.2202	13.4351
36.5911	22.9292	0.2435	15.0838
37.6441	22.9939	0.2506	15.4086

Table B.18, Data for m-xylene adsorption isotherm at 80 °C
(1st run, Desorption).

Pressures (Milibars)	Total mass (Miligrams)	Relative Pressure(P/Po)	Mass uptake % (($Wt - Wto)/Wto$)
37.6441	22.9939	0.250601	15.40863
35.9387	22.9118	0.239248	14.99656
32.9658	22.7434	0.219457	14.15135
29.9801	22.4426	0.199581	12.64160
26.9806	22.1746	0.179613	11.29648
23.9785	21.9826	0.159628	10.33282
20.9923	21.8377	0.139748	9.605549
17.9965	21.6973	0.119805	8.900868
15.0306	21.5444	0.100061	8.133448
12.0634	21.3783	0.080308	7.299776
9.1104	21.2034	0.060649	6.421935
6.0360	20.9799	0.040182	5.300167
3.0330	20.7226	0.020191	4.008753
1.0020	20.5091	0.006670	2.937176

Table B.19, Data for m-xylene adsorption isotherm at 80 °C
(2nd run, Adsorption).

Pressures (Milibars)	Total mass (Miligrams)	Relative Pressure(P/Po)	Mass uptake % (($Wt - Wto)/Wto$)
0.0000	19.9095	0.0000	0.0000
2.9893	20.0433	0.0199	0.6720
5.9860	20.1761	0.0398	1.3390
8.9785	20.3890	0.0597	2.4083
11.9843	20.7134	0.0797	4.0377
14.9958	21.0106	0.0998	5.5305
17.9934	21.2834	0.1197	6.9007
20.9967	21.5193	0.1397	8.0855
23.9900	21.7273	0.1597	9.1303
27.0315	21.9222	0.1799	10.1092
30.0611	22.1628	0.2001	11.3177
33.0858	22.5469	0.2202	13.2469
36.3550	22.8932	0.2420	14.9863
36.9155	22.9282	0.2457	15.1621

Table B.20 Data for m-xylene adsorption isotherm at 80 °C
(2nd run, Desorption).

Pressures (Milibars)	Total mass (Miligrams)	Relative Pressure(P/Po)	Mass uptake % (($Wt - Wto)/Wto$)
36.9155	22.9282	0.245751	15.16211
35.9376	22.8835	0.239241	14.93759
32.9815	22.6748	0.219562	13.88935
29.9749	22.3811	0.199547	12.41417
26.9839	22.1360	0.179635	11.18310
23.9790	21.9646	0.159631	10.32221
20.9939	21.8256	0.139759	9.624049
17.9932	21.6830	0.119783	8.907808
14.9972	21.5313	0.099838	8.145860
12.0433	21.3664	0.080174	7.317612
9.0895	21.1884	0.060510	6.423567
6.0174	20.9681	0.040059	5.317060
3.0392	20.7147	0.020232	4.044300
1.0021	20.5049	0.006671	2.990532

Table B.21, Data for o-xylene adsorption isotherm at 30 °C
(used sample, Adsorption).

Pressures (Milibars)	Total mass (Miligrams)	Relative Pressure(P/Po)	Mass uptake % $((Wt - Wto)/Wto)$
0.0000	19.9695	0.0000	0.0000
0.9841	20.2158	0.0833	1.2333
1.9748	20.4647	0.1672	2.4797
2.9743	20.6805	0.2519	3.5604
3.9740	20.8847	0.3366	4.5829
4.9762	21.0902	0.4215	5.6120
5.9757	21.2929	0.5062	6.6271
6.9744	21.4924	0.5908	7.6261
7.9798	21.6876	0.6759	8.6036
8.9747	21.8836	0.7602	9.5851
9.9688	22.1148	0.8444	10.7428
11.1379	22.6116	0.9434	13.2306

Table B.22, Data for o-xylene adsorption isotherm at 30 °C
(used sample, Desorption).

Pressures (Milibars)	Total mass (Miligrams)	Relative Pressure(P/Po)	Mass uptake % $((Wt - Wto)/Wto)$
11.1379	22.6116	0.943490	13.23068
10.0089	22.4108	0.847853	12.22514
9.0044	22.2486	0.762762	11.41290
7.9981	22.1139	0.677518	10.73838
6.9964	22.0014	0.592664	10.17502
5.9919	21.9026	0.507573	9.680262
5.0031	21.8006	0.423812	9.169483
4.0071	21.6860	0.339441	8.595608
3.0066	21.5587	0.254689	7.958136
2.0093	21.4137	0.170208	7.232029
0.9506	21.2315	0.080525	6.319637

Table B.23, Data for o-xylene adsorption isotherm at 30 °C
(fresh sample, Adsorption).

Pressures (Milibars)	Total mass (Miligrams)	Relative Pressure(P/Po)	Mass uptake % $((Wt-Wto)/Wto)$
0.0000	20.2117	0.0000	0.0000
0.9425	20.5181	0.0798	1.5159
1.9190	21.4727	0.1625	6.2389
2.8634	23.0657	0.2425	14.1205
3.9550	23.6216	0.3350	16.8709
4.9797	23.9033	0.4218	18.2646
5.9766	24.1149	0.5062	19.3115
6.9818	24.3023	0.5914	20.2387
7.9825	24.4750	0.6761	21.0932
8.9867	24.6463	0.7612	21.9407
9.9870	24.8225	0.8459	22.8125
11.1772	25.0552	0.9468	23.9638

Table B.24, Data for o-xylene adsorption isotherm at 30 °C
(fresh sample, Desorption).

Pressures (Milibars)	Total mass (Miligrams)	Relative Pressure(P/Po)	Mass uptake % $((Wt-Wto)/Wto)$
11.1772	25.0552	0.946819	23.96384
10.0173	24.9315	0.848564	23.35182
9.0116	24.8459	0.763371	22.92830
8.0099	24.7680	0.678518	22.54288
6.9950	24.6975	0.592546	22.19408
6.0112	24.6303	0.509208	21.86160
5.0134	24.5604	0.424684	21.51576
4.0149	24.4877	0.340102	21.15606
3.0230	24.4050	0.256078	20.74689
2.0193	24.3015	0.171055	20.23481
1.0151	23.7813	0.085989	17.66106

Table B.25, Data for o-xylene adsorption isotherm at 50 °C
(used sample, Adsorption).

Pressures (Milibars)	Total mass (Miligrams)	Relative Pressure(P/Po)	Mass uptake % $((Wt-Wto)/Wto)$
0.0000	19.4963	0.0000	0.0000
3.0033	19.6465	0.0892	0.7704
5.9948	19.8564	0.1780	1.8470
8.9750	20.2682	0.2666	3.9592
11.9336	21.2685	0.3545	9.0899
14.9259	22.6515	0.4434	16.1835
18.0372	22.9615	0.5358	17.7736
21.0290	23.1902	0.6247	18.9466
24.0784	23.3850	0.7153	19.9458
27.2710	23.5644	0.8101	20.8660
28.7449	23.6579	0.8539	21.3455
30.6099	23.9029	0.9093	22.6022

Table B.26, Data for o-xylene adsorption isotherm at 50 °C
(used sample, Desorption).

Pressures (Milibars)	Total mass (Miligrams)	Relative Pressure(P/Po)	Mass uptake % $((Wt-Wto)/Wto)$
30.6099	23.9029	0.909385	22.60224
29.0337	23.8284	0.862559	22.22011
27.2045	23.7436	0.808214	21.78516
23.9877	23.6607	0.712647	21.35995
20.9754	23.5925	0.623155	21.01014
17.9806	23.5228	0.534183	20.65264
14.9899	23.4464	0.445333	20.26077
11.9933	23.3563	0.356307	19.79863
9.03020	23.0461	0.268277	18.20756
6.07520	22.5476	0.180487	15.65066
3.11700	21.4725	0.092602	10.13628
1.01600	20.8709	0.030184	7.050569

Table B.27, Data for o-xylene adsorption isotherm at 50 °C
(fresh sample, Adsorption).

Pressures (Milibars)	Total mass (Miligrams)	Relative Pressure(P/Po)	Mass uptake % $((Wt-Wto)/Wto)$
0.0000	20.1839	0.0000	0.0000
2.9656	20.5404	0.0881	1.7662
5.9620	20.9564	0.1771	3.8273
8.9381	21.7435	0.2655	7.7269
11.8906	23.0367	0.3532	14.1340
14.9760	23.7435	0.4449	17.6358
18.0162	24.0067	0.5352	18.9398
21.0249	24.2137	0.6246	19.9654
24.0936	24.3896	0.7157	20.8369
27.1479	24.5553	0.8065	21.6578
29.2371	24.6528	0.8686	22.1409
30.6550	24.7023	0.91072	22.3861

Table B.28, Data for o-xylene adsorption isotherm at 50 °C
(fresh sample, Desorption).

Pressures (Milibars)	Total mass (Miligrams)	Relative Pressure(P/Po)	Mass uptake % $((Wt-Wto)/Wto)$
30.6550	24.7023	0.910725	22.38616
28.9578	24.6631	0.860303	22.19195
26.9768	24.6201	0.801450	21.97890
23.9859	24.5521	0.712594	21.64200
21.0112	24.4843	0.624219	21.30609
18.0184	24.4112	0.535306	20.94392
15.0170	24.3309	0.446138	20.54608
12.0474	24.2310	0.357914	20.05113
9.1084	23.8390	0.270600	18.10899
6.0760	23.3229	0.180511	15.55200
3.0521	22.2276	0.090674	10.12540
1.0086	21.6997	0.029964	7.509946

Table B.29, Data for o-xylene adsorption isotherm at 65 °C
(used sample, Adsorption).

Pressures (Milibars)	Total mass (Miligrams)	Relative Pressure(P/Po)	Mass uptake % $((Wt-Wto)/Wto)$
0.0000	19.4158	0.0000	0.0000
2.9976	19.5438	0.0446	0.6592
5.9858	19.7369	0.0891	1.6538
9.0080	20.1832	0.1342	3.9524
11.9945	20.7194	0.1787	6.7141
14.9959	21.1932	0.2234	9.1544
17.9785	22.0601	0.2678	13.619
21.0082	22.5490	0.3129	16.1373
24.1088	22.7263	0.3591	17.0505
27.3146	22.8711	0.4069	17.7963
28.9816	22.9320	0.4317	18.1099
30.6726	22.9809	0.4569	18.3618

Table B.30, Data for o-xylene adsorption isotherm at 65 °C
(used sample, Desorption).

Pressures (Milibars)	Total mass (Miligrams)	Relative Pressure(P/Po)	Mass uptake % $((Wt-Wto)/Wto)$
30.6726	22.9809	0.456982	18.36185
28.9575	22.9491	0.431429	18.19807
26.9706	22.9087	0.401827	17.98999
23.9790	22.8425	0.357256	17.64903
20.9833	22.7300	0.312624	17.06960
17.9868	22.5924	0.267980	16.36090
14.9956	22.2598	0.223415	14.64786
11.9912	21.7777	0.178653	12.16483
8.9873	21.2024	0.133899	9.201784
6.0327	20.8805	0.089879	7.543856
3.1397	20.5573	0.046777	5.879232
1.0394	20.2489	0.015486	4.290835

Table B.31, Data for o-xylene adsorption isotherm at 65 °C
(fresh sample, Adsorption).

Pressures (Milibars)	Total mass (Miligrams)	Relative Pressure(P/Po)	Mass uptake % $((Wt-Wto)/Wto)$
0.0000	20.0991	0.0000	0.0000
2.9890	20.3369	0.0445	1.1831
5.9770	20.6585	0.0890	2.7832
8.9811	21.2542	0.1338	5.7470
11.9862	21.8145	0.1785	8.5347
14.9845	22.3035	0.2232	10.9676
17.9891	23.1312	0.2680	15.0857
20.9954	23.5893	0.3128	17.3649
24.0086	23.7629	0.3576	18.2286
27.0539	23.9045	0.4030	18.9331
28.9597	23.9693	0.4314	19.2555
30.6258	24.0173	0.4562	19.4944

Table B.32, Data for o-xylene adsorption isotherm at 65 °C
(fresh sample, Desorption).

Pressures (Milibars)	Total mass (Miligrams)	Relative Pressure(P/Po)	Mass uptake % $((Wt-Wto)/Wto)$
30.6258	24.0173	0.456284	19.49441
28.9591	23.9814	0.431453	19.31579
26.9710	23.9430	0.401833	19.12474
23.9857	23.8577	0.357355	18.70034
20.9901	23.7297	0.312725	18.06350
18.0182	23.5653	0.268448	17.24555
15.0328	23.2294	0.223969	15.57433
12.0680	22.6438	0.179797	12.66077
9.1570	22.1977	0.136427	10.44126
6.0631	21.8598	0.090332	8.760094
3.0470	21.4475	0.045396	6.708758
1.0324	21.0956	0.015381	4.957933

Table B.33, Data for o-xylene adsorption isotherm at 80 °C
(used sample, Adsorption).

Pressures (Milibars)	Total mass (Miligrams)	Relative Pressure(P/Po)	Mass uptake % $((Wt - Wto)/Wto)$
0.0000	19.3157	0.0000	0.0000
2.9968	19.4268	0.0239	0.5751
5.9875	19.5799	0.0479	1.3677
8.9952	19.8765	0.0719	2.9033
12.0005	20.1778	0.0960	4.4632
15.0141	20.4574	0.1201	5.9107
18.0197	20.7062	0.1441	7.1988
21.0214	20.9358	0.1681	8.3874
24.0666	21.1614	0.1925	9.5554
27.1596	21.5457	0.2172	11.5450
28.9889	21.8162	0.2319	12.9454
30.6776	22.0040	0.2454	13.9176

Table B.34, Data for o-xylene adsorption isotherm at 80 °C
(used sample, Desorption).

Pressures (Milibars)	Total mass (Miligrams)	Relative Pressure(P/Po)	Mass uptake % $((Wt - Wto)/Wto)$
30.6776	22.0040	0.24544	13.9176
28.9740	21.8578	0.23181	13.1608
26.9792	21.6184	0.21585	11.9213
23.9829	21.3119	0.19187	10.3346
20.9885	21.1097	0.16792	9.28778
17.9896	20.9556	0.14392	8.48998
14.9952	20.8008	0.11997	7.68856
11.9923	20.6319	0.09594	6.81414
9.0461	20.4537	0.07237	5.89158
6.1059	20.2650	0.04885	4.91465
3.0363	20.0323	0.02429	3.70993
1.0054	19.8505	0.00804	2.76873
0.4144	19.7898	0.00331	2.45448

Table B.35, Data for o-xylene adsorption isotherm at 80 °C
(fresh sample, Adsorption).

Pressures (Milibars)	Total mass (Miligrams)	Relative Pressure(P/Po)	Mass uptake % $((Wt-Wto)/Wto)$
0.0000	20.0592	0.0000	0.0000
2.9886	20.2308	0.0239	0.8554
5.9856	20.4344	0.0478	1.8704
8.9854	20.7787	0.0718	3.5868
11.994	21.1172	0.0959	5.2743
14.991	21.4100	0.1199	6.7340
18.015	21.6714	0.1441	8.0372
21.038	21.8997	0.1683	9.1753
24.070	22.1360	0.1925	10.3533
27.140	22.4483	0.2171	11.9102
29.254	22.7368	0.2340	13.3484
30.689	22.8914	0.2455	14.1192

Table B.36, Data for o-xylene adsorption isotherm at 80 °C
(fresh sample, Desorption).

Pressures (Milibars)	Total mass (Miligrams)	Relative Pressure(P/Po)	Mass uptake % $((Wt-Wto)/Wto)$
30.6895	22.8914	0.245536	14.11921
28.9669	22.7153	0.231754	13.24131
26.9748	22.5034	0.215816	12.18493
23.9955	22.2606	0.191979	10.97452
21.0107	22.0907	0.168099	10.12752
18.0127	21.9342	0.144113	9.347332
15.0061	21.7698	0.120058	8.527758
12.0732	21.6014	0.096593	7.688243
9.13040	21.4067	0.073049	6.717616
6.05990	21.1813	0.048483	5.593942
3.04100	20.9147	0.024330	4.264876
1.02600	20.6990	0.008209	3.189559

Table B.37, Data for ethylbenzene adsorption isotherm at 30°C (Adsorption).

Pressures (Milibars)	Total mass (Miligrams)	Relative Pressure(P/Po)	Mass uptake % $((Wt - Wto)/Wto)$
0.0000	19.8510	0.0000	0.0000
0.9327	20.3402	0.0524	2.4643
1.9758	20.5101	0.1111	3.3202
2.9735	20.6670	0.1672	4.1106
3.9731	20.8311	0.2235	4.9372
4.9642	21.0048	0.2792	5.8123
5.9514	21.2009	0.3348	6.8001
6.9514	21.4237	0.3910	7.9225
7.9558	21.6912	0.4475	9.2700
8.9238	22.0436	0.5020	11.0452
9.8539	22.9122	0.5543	15.4208
10.8798	23.5177	0.6120	18.4711
11.9202	23.7359	0.6705	19.5703
12.9356	23.9080	0.7277	20.4372
13.9451	24.0573	0.7844	21.1893
14.9493	24.1906	0.8409	21.8608
15.9536	24.3135	0.8974	22.4799

Table B.38, Data for ethylbenzene adsorption isotherm at 30°C (Desorption).

Pressures (Milibars)	Total mass (Miligrams)	Relative Pressure(P/Po)	Mass uptake % $((Wt - Wto)/Wto)$
15.9536	24.3135	0.89748	22.47998
14.9857	24.2830	0.84303	22.32633
13.9919	24.2489	0.78712	22.15455
12.9926	24.2153	0.73090	21.98529
11.9918	24.1774	0.67460	21.79437
10.9911	24.1410	0.61831	21.61100
9.9954	24.1014	0.56229	21.41152
8.9916	24.0577	0.50582	21.19138
7.9928	24.0131	0.44964	20.96670
6.9941	23.9624	0.39345	20.71130
5.9928	23.8503	0.33712	20.14659
5.0177	23.6817	0.28227	19.29726
4.0246	23.4513	0.22640	18.13662
3.0294	23.1369	0.17042	16.55282
2.0509	22.6059	0.11537	13.87789
0.9780	22.0944	0.05501	11.30119

Table B.39, Data for ethylbenzene adsorption isotherm at 65°C (Adsorption).

Pressures (Milibars)	Total mass (Miligrams)	Relative Pressure(P/Po)	Mass uptake % (($Wt - Wto$)/Wto)
0.0000	20.0964	0.0000	0.0000
3.0236	20.2576	0.0324	0.8021
5.9988	20.6074	0.0644	2.5427
8.9881	21.1541	0.0965	5.2631
11.9776	21.5900	0.1286	7.4321
15.9681	22.1384	0.1715	10.1610
19.9719	22.9729	0.2145	14.3135
23.9431	23.3870	0.2572	16.3740
27.9431	23.5566	0.3002	17.2180
31.9326	23.6988	0.3430	17.9256
35.9527	23.8266	0.3862	18.5615
39.9922	23.9406	0.4296	19.1288

Table B.40, Data for ethylbenzene adsorption isotherm at 65°C (Desorption).

Pressures (Milibars)	Total mass (Miligrams)	Relative Pressure(P/Po)	Mass uptake % (($Wt - Wto$)/Wto)
39.9922	23.9406	0.429654	19.1288
35.9126	23.8693	0.385825	18.7740
31.9432	23.7995	0.343180	18.4266
27.9613	23.7172	0.300401	18.0171
23.9820	23.5478	0.257649	17.1742
19.9913	23.3750	0.214775	16.3143
15.9942	23.0018	0.171833	14.4573
12.0917	22.3642	0.129907	11.2846
8.9953	21.8929	0.096641	8.93941
5.9924	21.5672	0.064379	7.31872
2.9731	21.1612	0.031941	5.29846
0.9802	20.8236	0.010531	3.61855

Table B.41, Data for ethylbenzene adsorption isotherm at 80°C
(1st run, Adsorption).

Pressures (Milibars)	Total mass (Miligrams)	Relative Pressure(P/Po)	Mass uptake % $((Wt - Wto)/Wto)$
0.0000	19.9099	0.0000	0.0000
2.9726	20.1980	0.0176	1.4470
5.9608	20.5379	0.0353	3.1542
8.9701	20.8171	0.0531	4.5565
11.9645	21.0567	0.0709	5.7599
15.9629	21.3460	0.0946	7.2129
19.9450	21.5970	0.1182	8.4736
23.9232	21.8271	0.1418	9.6293
27.9323	22.0951	0.1655	10.9754
31.9211	22.5611	0.1892	13.3159
35.9291	22.9125	0.2129	15.0809
39.9364	23.1457	0.2367	16.2522

Table B.42, Data for ethylbenzene adsorption isotherm at 80°C
(1st run, Desorption).

Pressures (Milibars)	Total mass (Miligrams)	Relative Pressure(P/Po)	Mass uptake % $((Wt - Wto)/Wto)$
39.9364	23.1457	0.23675	16.2522
35.9407	22.9417	0.21306	15.2276
31.9627	22.6911	0.18948	13.9689
27.9538	22.2733	0.16571	11.8704
23.9632	21.9724	0.14205	10.3591
19.9827	21.7646	0.11846	9.31546
15.9985	21.5603	0.09484	8.28934
11.9960	21.3328	0.07111	7.14669
8.9933	21.1431	0.05331	6.19390
5.9948	20.9234	0.03553	5.09043
3.0099	20.6687	0.01784	3.81116
0.9955	20.4608	0.00590	2.76696

Table B.43, Data for ethylbenzene adsorption isotherm at 80°C
(2nd run, Adsorption).

Pressures (Milibars)	Total mass (Miligrams)	Relative Pressure(P/Po)	Mass uptake % $((Wt - Wto)/Wto)$
0.0000	19.9692	0.0000	0.0000
3.0170	20.1107	0.0178	0.7085
5.9869	20.4801	0.0354	2.5584
8.9843	20.7956	0.0532	4.1383
11.9905	21.0592	0.0710	5.4584
15.9776	21.3664	0.0947	6.9967
19.9651	21.6275	0.1183	8.3042
23.9512	21.8687	0.1419	9.5121
27.9384	22.1779	0.1656	11.0605
31.9344	22.6674	0.1893	13.5118
35.9429	22.9783	0.2130	15.0687
40.0086	23.2480	0.2371	16.4192

Table B.44, Data for ethylbenzene adsorption isotherm at 80°C
(2nd run, Desorption).

Pressures (Milibars)	Total mass (Miligrams)	Relative Pressure(P/Po)	Mass uptake % $((Wt - Wto)/Wto)$
40.0086	23.2480	0.237178	16.41929
35.9350	23.0219	0.213029	15.28704
31.9507	22.8045	0.189409	14.19837
27.9748	22.4059	0.165839	12.20229
23.9717	22.0398	0.142108	10.36897
19.9948	21.8106	0.118533	9.221201
16.0197	21.5977	0.094968	8.155059
12.3594	21.3921	0.073269	7.125473
9.0589	21.1744	0.053703	6.035294
6.0513	20.9541	0.035873	4.932095
3.0620	20.6944	0.018152	3.631593
1.0465	20.4816	0.006204	2.565952

APPENDIX C

ANTOINE EQUATION AND HISTORY WORK OF MCM-41 SAMPLE

C.1 Antoine equation

$$\log_{10} p = A - B / (T + C)\ldots\ldots\ldots\ldots\ldots\ldots\ldots(C.1)$$

Pressure in mmHg, T in degrees Celsius, A, B, C are Antoine coefficient which were adapted from [65] for all sorbates.

Table C.1, Antoine coefficients for the sorbates adapted from [65].

Sorbate	Coefficient A	Coefficient B	Coefficient C	Temperature Range (°C)
p-xylene	7.15471	1553.95	225.230	13.26 – 343.11
m-xylene	7.18115	1573.02	226.671	(- 47.85) – 343.90
o-xylene	7.14914	1566.59	222.596	(- 25.17) – 357.22
Ethylbenzene	7.15610	1559.55	228.582	(- 94.95) – 344.02

Table C.2, Vapour pressure of sorbates at adsorption temperatures (calculated by Antoine equation).

Sorbate	Vapour pressure at 30°C (Milibars)	Vapour pressure at 50°C (Milibars)	Vapour pressure at 65°C (Milibars)	Vapour pressure at 80°C (Milibars)	Critical temperature (°C)
p-xylene	15.530	42.811	84.219	153.768	343.11
m-xylene	15.049	41.738	81.832	150.215	343.90
o-xylene	11.805	33.660	67.120	124.990	357.22
ethylbenzene	17.776	48.176	93.080	168.686	344.02

C.2 History of MCM-41 samples

Table C.3, History of the first MCM-41 sample

Sorbate	Run at 30°C	Run at 50°C	Run at 65°C	Run at 80°C
p-xylene	?	1st run	2nd run	3rd run
p-xylene	?	?	?	4th run
m-xylene	5th run	6th run	7th run	8th run
m-xylene	?	?	?	9th run
o-xylene	10th run	11th run	12th run	13th run

Table C.4, History of the second MCM-41 sample

Sorbate	Run at 30°C	Run at 50°C	Run at 65°C	Run at 80°C
o-xylene	1st run	2nd run	3rd run	4th run
Ethylbenzene	5th run	?	6th run	7th run
Ethylbenzene	?	?	?	8th run
p-xylene	9th run	?	?	?

C.3 Clausius-Clapeyron equation

$$Ln\ P = \frac{\Delta Hvap}{RT} + C$$

…………………………………………………………...(C.3)

Where P and T are the equilibrium pressure and temperature, R is the gas constant, C is a constant.

APPENDIX D

INTELLIGENCE GRAVIMETRIC ANALYSER

D.1 Intelligence gravimetric analyser (IGA system)

D.1.1 IGA-001- Gas sorption system

The model IGA-001 system is designed to study the gas sorption properties of materials. This system forms the core of the IGA range of gravimetric analysers. The IGA design integrates precise computer-control and measurement of weight change, pressure and temperature to enable fully automatic and reproducible determination of gas adsorption-desorption isotherms and isobars in diverse operating conditions.

D.1.2 IGA-002 – Vapour sorption system

The model IGA-002 system is specifically designed to study water and vapour sorption. The system is available in a high vacuum configuration to enable microporous materials to be studied. A selection of pressure sensors enables pressure control at very low partial vapour pressures. The incorporated anti-condensation system extends the temperature range to 50°C over which the full *P/Po* envelope can be measured. This system was used for our work.

D.1.3 IGA-003 –Dynamic sorption system

The model IGA-003 system is specifically designed for experimental applications where it is necessary to have a dynamic flow of gas past the sample (the determination of multi-component isotherms for example). In this arrangement it is possible to have up to four gas streams mixed

prior to entry in to IGA system so that a defined composition is delivered at the sample position.

D.2 Loading MCM-41 sample

IGA software guides us through the procedure for sample loading. This is initiated either by clicking with the left hand mouse button on the **New sample** tool, which is at the far left of the Tool bar, or by selecting **File, New sample** from the menu. The first stage of the sample loading is to enter the current system password in the message box that will appear after that we select **New sample** tool. The IGA software will be in idle mode after **New sample** tool and our next action will depend on whether we need to reconfigure the IGA system. The sorbate used in the experiment must have corresponding entries in the IGA gas database which is viewed and created by the selection **Setup, Gas** while the IGA is still in idle mode. Sample loading also requires the data for buoyancy corrections which defined in chapter 2 in IGA systems user manual [64].

D.2.1 Gas setup tool

Gas setup stores sorbate data but is not used to change sorbate which can only achieved using **New Application** tool.

When a new sorbate is used the associated physical properties also need to be entered in the IGA gas database and this is achieved by selecting **Setup, Gas** while IGASwin is idling. We can also review and change properties of existing species by selecting the Gas setup button when available during **New Application**. Not all the information is compulsory as some parameters are solely for data reductions and analyses that we may not require. Gas setup is a window with four categories:

1- **General**: which include the name of the sorbate, if it is hazard or not, chemical name, formula, description and molar mass which is compulsory parameter.

2- **Compressibility**: at high gas pressure and / or low gas temperature, the buoyancy correction (appendix B in IGA system user manual) is increasingly sensitive to the calculated gas density and therefore to the gas compressibility factor.

3- **Vapour phase**: the distinction between gas and vapour species is defined by the critical temperature which is the first parameter of this category. Any measurement below this temperature may require definition of the vapour pressure, (Po), for two reasons: firstly, to prevent condensation in the chamber due to over-pressure and, secondly, to enable calculation of relative pressure, *P/Po* at the sample. In the first instance the system will automatically trip if severe condensation occurs since the pressure controller cannot attain the set-point and the failure is equivalent to exhaustion of the sorbate supply and is the measurement will stop at this point. If the software calculates, Po, from the measured operating conditions then this condition is avoided and, for example during isothermal measurements the scan reverses from adsorption to desorption. This only strictly applies if the saturation vapour pressure is lower than the maximum operating pressure for the current instrument configuration. In the second case the definition of P/Po during the measurement and as the fundamental scale for comparing uptake is a normal requirement for measurement of the vapour phase.

The protection against condensation is generally referred to as a part of the IGA "Anti-condensation protection" and operates in conjunction with thermostats and temperature sensors to define and measure the temperature of the chamber. The critical temperature (T_c °C) defines when anti-condensation protection is

applied and is the threshold for the vapour pressure calculation using all the other parameters of this category. This is a compulsory parameter for the vapours and will enable the calculations for vapour pressure. The value may also be used in compressibility calculations. The software provides definition by one of three vapour pressure equations. The first equation which is the one we used in our experiments was Antoine equation (see Appendix C)

4- **Sorbate phase:** (Appendix B in IGA system user manual).

D.2.2 New Application tool

New application changes the IGA configuration in any or all of the following ways:

1- Configuration of the pressure controller (IGA-003, IGA-002)

2- Source of the gas/vapour supply(IGA-002, IGA-002/3)

3- Choice of reactor (and therefore the operating pressure and temperature limit) if more than one option is available.

4- Choice of thermostat if more than one option is available.

5- Definition of the sorbate species and connection of the sorbate supply.

6- Choice of the pressure sensor used for the experiment if IGA has more than one.

If we are about to carry out an experiment for the first time with new sorbate species then first we should check that this species appears in the gas database. If not we should enter the information related to sorbate in the database (see gas setup tool).

The first choice during **New application** tool is the pressure control. For our work the choice is 'static' mode. Which is control of a single component gas or vapour species. Control is not static in most (regulated) application unless the sample is in isothermal equilibrium (i.e., there will be some flow of gas into or out of the IGA chamber to maintain constant pressure).

The second option is the source of gas or vapour species. For our work was liquid reservoir.

The third option is the choice of IGA reactor. For our work the selection was SS 316N reactor.

The fourth option is the choice of thermostat. For our work the selection was furnace. Bear in mind that this will set temperature limit for sample pre-treatment and for regeneration for the MCM-41 sample.

Then we should select our sorbate and after that the desired pressure range. For our work which was 100 mbar.

Table D.1, IGA-002 valve Position for static mode gas pressure set (Idle mode).

Valve	Symbol	Position
PIV1		Closed
PIV2 high Pressure Expt.		Closed B Pressure Range P1
PIV2 low Pressure Expt.		Open A Pressure Range P2 Pressure Range P3 Pressure Range Auto
PIV3		Horizontal(closed)
PIV4		Left
PIV5		Up
PIV6		Horizontal(closed)
EV1		Horizontal(closed)
EV2		Vertical(closed)
EV3		Down
Air Admit		Closed

D.3 The valves and devices shown in all process schematics within this section are defined as follows:

PIV1   High conductance exhaust valve
PIV2   P2/P3 sensor isolation valve
PIV3   Static-dynamic inlet mode valve
PIV4   Gas-vapour mode valve
PIV5   Static-dynamic exhaust mode valve
PIV6   Counter flow isolation valve

MV1   Admittance control valve
MV2   Exhaust control valve

EV1   Vacuum block-bleed valve
EV2   DSMS isolation valve
EV3   Turbo pump air admittance valve

P1   Primary pressure sensor
P2   Second pressure sensor
P3   Third pressure sensor

LR   Liquid reservoir
V1   IGA vacuum gauge
V2   DSMS vacuum gauge

VENT1 Chamber over-pressure safety valve
VENT2 Liquid reservoir over-pressure safety valve(glass reservoir only)
VENT3 P2/P3 over-pressure safety valve
VENT4 Pump manifold over-pressure safety valve
VENT5 Optional DSMS inlet over-pressure safety valve

D1   DSMS inlet isolation valve
D2   DSMS bypass pump isolation/throttle valve
D3   DSMS auto air admittance valve